Excitation-Energy Sharing in the Reaction $^{51}V + ^{197}Au$ at the Barrier [B]

P.Klein[1], W.Brüchle[2], M.K.Gober[1], J.V.Kratz[1], M.Schädel[2], H.P.Zimmermann[1]
[1]Institut für Kernchemie, Universität Mainz, [2]GSI Darmstadt

The excitation-energy sharing among the reaction products contains important information about the intrinsic equilibration process in heavy-ion collisions. Deviations from the thermal equilibrium with an excitation-energy division proportional to the ratio of the fragment masses have been observed repeatedly, in particular for the early equilibration phase. Also for low dissipated energies, an extreme dependence of the excitations-energy division on the mass flow was observed[1]. For quasi-fission reactions characterized by the complete damping of the kinetic energy and by large mass and charge transfer, one might expect that thermal equilibrium is reached. However, we have previously[2,3] observed cold target-like fragments and highly excited projectile-like fragments in quasi-fission reactions at the barrier.

Our previous experiments[2,3] were restricted to observing the mass flow from the target to the projectile. In order to test a possible dependence of the excitation-energy division on the direction of the mass flow we looked also at the below-projectile and trans-target products in the reaction $^{51}V + ^{197}Au$. The experiments were carried out at the Bass-model Coulomb barrier E_{BASS} (E_{Lab}=4.86 MeV/u) where projectile and target touch each other with relative velocity v=0. In addition, in order to introduce a friction force, the bombarding energy was increased by 25 MeV in the cm system (E_{Lab}=5.48 MeV/u) in a second experiment. The reaction products, after being stopped in 4π geometry in catcher foils, were subject to extensive chemical separations and low-level γ-ray spectroscopy over a period of several weeks.

The resulting cross sections are used to define centroids $\langle A\rangle_Z^{sec}$ of the isotope distribution for given elements. These post-neutron emission centroids are compared with pre-neutron emission centroids $\langle A\rangle_Z^{prim}$ calculated by using the minimum potential energy concept. The resulting missing mass is used to determine the average excitation energy as a function of Z with the help of evaporation calculations:

$$\langle A\rangle_Z^{prim} \xrightarrow[\text{missing mass}]{\langle\nu\rangle_Z} \langle A\rangle_Z^{sec} \qquad \downarrow \qquad \langle E^*\rangle_Z$$

The results are given in Fig.1 ($E_{CM}=E_{BASS}$) and in Fig.2 ($E_{CM}=E_{BASS}$+25 MeV).

Fig.1 shows that the extreme acceptor-donor asymmetry observed earlier in reactions where the bombarding energy corresponds exactly to the barrier is reproduced. For the first time, this observation is also made for channels with net mass transfer towards larger asymmetry.
Products lighter than the projectile are formed relatively cold, and products heavier than the target are carrying increasingly large excitation energies.
Fig.2 shows that the acceptor-donor asymmetry is much less pronounced if the bombarding energy is increased by only 25 MeV above the barrier, and that there is a trend towards equal energy sharing.

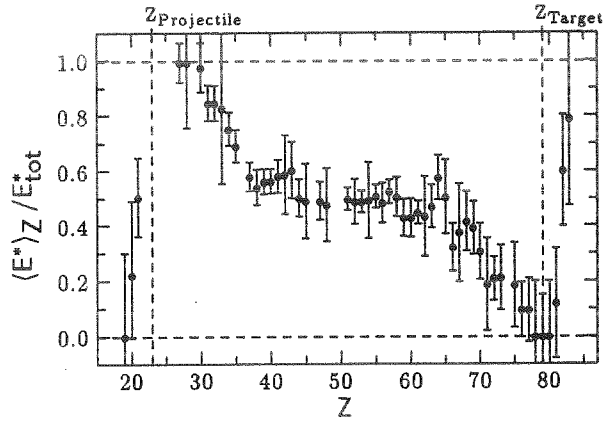

Fig.1: Division of the total excitation energy at E_{Lab}=4.86 MeV/u (E_{BASS})

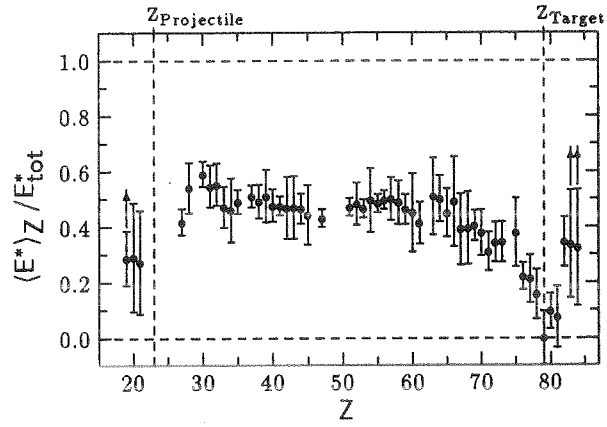

Fig.2: Division of the total excitation energy at E_{Lab}=5.48 MeV/u (E_{BASS}+25 MeV)

We suggest that the observed sharing of excitation energy at the barrier has a common origin with the 'sawtooth' phenomenon in low-energy fission, namely shape fluctuations at scission. The result is a dependence of the excitation-energy sharing on the direction of the mass flow. Already at a slightly higher bombarding energy the excitation energy division due to shape fluctuations is covered up by the dissipation of extra relative kinetic energy via nucleon exchange[4]. Attempts to quantitatively reproduce the experimental results by the 'random neck rupture' model[5] are under way.

[1]H.Sohlbach et al., Phys.Lett. 153B, 386 (1985)
[2]H.Keller et al., Z.Phys. A328, 255 (1987)
[3]H.Gäggeler et al., Phys.Rev. C33,1983 (1986)
[4]J.Randrup, Nucl.Phys. A307, 319 (1978); A327, 490 (1979); A383, 468 (1982)
[5]U.Brosa et al., Phys.Rep. 197, 167 (1990)

Z-Distributions and Reaction Components in the $^{51}V + ^{197}Au$ Reaction [B]

P.Klein[1], W.Brüchle[2], M.K.Gober[1], J.V.Kratz[1], M.Schädel[2], H.P.Zimmermann[1]
[1]Institut für Kernchemie, Universität Mainz, [2]GSI Darmstadt

Integrals of the Gaussian isotope distributions[1,2] of the binary reaction products (except for the quasi-elastic reaction component which is confined to a very narrow range of Z and A values around the entrance channel values and which is eliminated) are shown in Figs. 1 and 2 for $^{51}V + ^{197}Au$ collisions at the Bass-model barrier and 25 MeV above the barrier, respectively. As charged-particle evaporation can be ignored, the Z-distributions should be symmetric about $(Z_1 + Z_2)/2 = 51$. Therefore, we have reflected the Z-yields at Z=51 so that twice as many data points appear in Figs. 1 and 2 than are measured. This should help to weaken the influence of systematic errors on individual Z-yields (due to e.g. systematic errors in the chemical yield determination) on the definition of the smooth dependence of the cross sections on Z. The gross features of the total Z-distributions are as follows: At both energies near Z=23 and 79, there is a relatively narrow distribution of "deep-inelastic" reaction products, with a slight tail towards symmetry, FWHM=4.8 at $E_{CM}=E_{BASS}$ and FWHM=5.3 at $E_{CM}=E_{BASS}$+25 MeV. At the lower energy, there is a broad flat plateau of cross sections, or maybe a shallow minimum, between these "deep-inelastic" peaks. At the higher energy, a broad maximum at symmetry is evident which is indicative of the appearance of a fusion-fission component. The solid lines are an attempt to subdivide the total distribution into its constituent contributions - a "deep-inelastic" component, a quasi-fission component, and the fusion-fission component. The asymmetric bumps peaking near Z=30 and Z=70 have shapes that are based on analyses[3,4] of the mass-angle correlations in quasi-fission reactions. The width of the fusion-fission distribution (FWHM$\simeq$20) is compatible with systematics[5]. The fusion-fission component shown in Fig. 1 is the maximum possible contribution compatible with the data of this energy. A fit without a fusion-fission component is of equal quality.

The increase of the fusion-fission cross section with bombarding energy is compatible with the extra-push systematics[6] which predicts a barrier shift (E_B-E_{BASS})=18 MeV and a barrier fluctuation σ_B=8.7 MeV. Note that the relative importance of the quasi-fission reactions also increases with increasing bombarding energy. At $E_{CM}=E_{BASS}$, the peak-to-valley ratio (peak of the "deep-inealstic" distribution) is about 7:1, at E_{BASS}+25 MeV, the ratio decreases to about 4:1.

The decomposition of the total Z-distribution in its constituent components is important for the comparison of the excitation energy sharing[2,7] in this reaction with predictions of the 'random neck rupture' model[8]. In this model, different pre-scission shapes are associated with different mass distributions: A short symmetric pre-scission shape gives a narrow mass distribution at symmetry (fusion-fission). A modestly asymmetric pre-scission shape gives the quasi-fission bumps and the excitation energy division exhibits a sawtooth-like form. The "deep-inelastic" peaks are associated with strongly asymmetric pre-scission shapes and an extremely steep sawtooth that also seems to be required by the data[7] near Z=23 and Z=79.

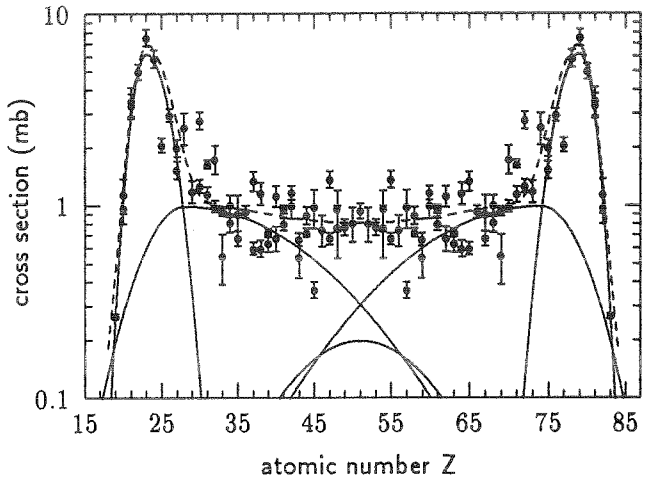

Fig.1: Z-distribution and its decomposition into "deep-inelastic", quasi-fission, and fusion-fission components at $E_{CM}=E_{BASS}$

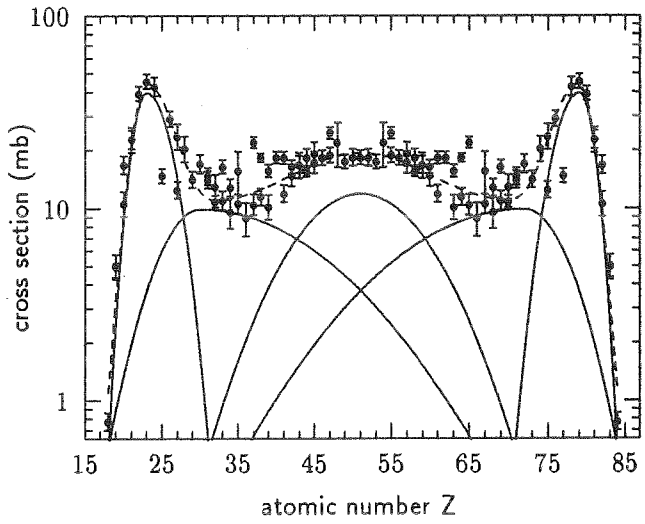

Fig.2: Z-distribution and its decomposition into "deep-inelastic", quasi-fission, and fusion-fission components at $E_{CM}=E_{BASS}$+25 MeV

[1]M.K.Gober et al., contribution to this report
[2]P.Klein, Dissertation, Universität Mainz (1993)
[3]R.Bock et al., Nucl.Phys. A388, 334 (1982)
[4]J.Töke et al., Nucl.Phys. A440, 327 (1985)
[5]C.C.Sahm et al., Z.Phys. A297, 241 (1980)
[6]A.B.Quint et al., Z.Phys.A, in press
[7]P.Klein et al., contribution to this report
[8]U.Brosa et al., Nucl.Phys. A502, 423 (1989)

Production of Lanthanides in the Reaction $^{51}V + ^{197}Au$ ^{B}

M.K. Gober[1], P. Klein[1], J.V. Kratz[1], W. Brüchle[2], M. Schädel[2]
[1] Institut für Kernchemie der Universität Mainz, [2]GSI Darmstadt

Production rates and isotopic distributions of Yttrium, Lanthanum and the Lanthanides (Rare Earth Elements, REE) in the reaction $^{51}V + ^{197}Au$ at the Bass-model barrier, $E_{cm} \equiv B$, and $E_{cm} = B + 25$ MeV were determined. The reaction products were collected in a copper catcher foil and separated in an extensive chemical procedure [1] after the irradiations yielding about 20 fractions.

Yttrium and the REE were isolated and separated in five fractions, F1 - F5, by means of cation exchange chromatography. The samples were prepared by coprecipitation with $Fe(OH)_3$. Special precautions had to be taken to minimize contamination with sodium to reduce the background in the neutron activation measurements performed for determination of the chemical yield [2].

γ-counting started immediately after the end of separation and lasted for 2 months. 16 calibrated low-level-Ge(Li)-detectors were used. The spectra were transferred to the IBM, the evaluation was done off-line by using the code GAMANAL. For halflife analysis and nuclide identification, the TCL-program package was used. Finally, the determined activities at the end of irradiation were converted to production rates by the program BEAM. The calculated cross sections had to be corrected for the chemical yield, the target thickness, the catcher foil geometry and the decay and growth of precursor nuclides [2].

As mentioned above, the chemical yields of the REE were determined by instrumental neutron activation analysis (INAA). Prior to the chemical separations μg-amounts of inactive carriers had been added. After the end of the γ-measurements, the samples were irradiated in the TRIGA Mainz and their count rates were compared with standards prepared and irradiated unter the same conditions. The chemical yields are shown in Tab. 1:

	VAU1	VAU2a	VAU2b	VAU3
E	1.00 x B	1.00 x B	1.00 x B	1.13 x B
Lu	56.3%	42.1%	76.7%	45.4%
Yb	71.1%	63.0%	74.8%	75.8%
Tm	67.2%	66.2%	54.5%	52.8%
Er	75.9%	62.6%	F1: 17.2%	58.9%
			F2: 59.9%	24.8%
Ho	86.7%	100%	85.4%	84.2%
Y	37%	74%	64%	67%
Dy	F3: 80.2%	84.2%	F2: 23.3%	38.9%
	F4: 0.5%		F2: 82.0%	54.5%
Tb	75.3%	71.0%	91.2%	96.5%
Gd	73.3%	69.2%	82.0%	89.8%
Eu	87.0%	93.5%	99.1%	92.8%
Sm	75.0%	F3: 1.4%	10.6%	24.2%
		F4: 90.4%	63.3%	49.7%
Pm	42%	36%	45%	65%
Nd	F4: 82.1%	78.9%	86.5%	100%
	F5: 23.7%			
Pr	79.1%	67.7%	62.9%	59.7%
Ce	68.7%	58.1%	69.8%	71.3%
La	60.7%	29.3%	36.6%	43.5%

Table 1: Chemical Yields for the REE in the reaction $^{51}V + ^{197}Au$.

The isotopic distributions in the lanthanide region are shown in Fig. 1. The Gaussians fitted to the data have a width (FWHM) of 4.5 mass units, this is the same value as for all other elements up to Os and down to Co. For products heavier than Os and lighter than Co, the width decreases to 4.0 mass units, an indication for a change in the production mechanism, see Refs. [3, 4]. The REE cross sections complete the cross section systematics obtained for all other elements from K up to Po [3, 4]. They serve two purposes:

i) the centroids of the isotopic distributions for each element are used to deduce the average fractional excitation energy E^*_Z / E^*_{tot}, and

ii) the integrals of the Gaussians are used to define complete Z distributions and their decomposition into deep-inelastic transfer, quasi-fission, and fusion-fission components. This is the subject of two accompanying contributions to this report [3].

[1] P. Klein, Diploma Thesis, Universität Mainz 1989
[2] M.K. Gober, Doctoral Thesis, Universität Mainz 1992
[3] P. Klein et al., contribution to this report
[4] P. Klein, Doctoral Thesis, Universität Mainz 1993

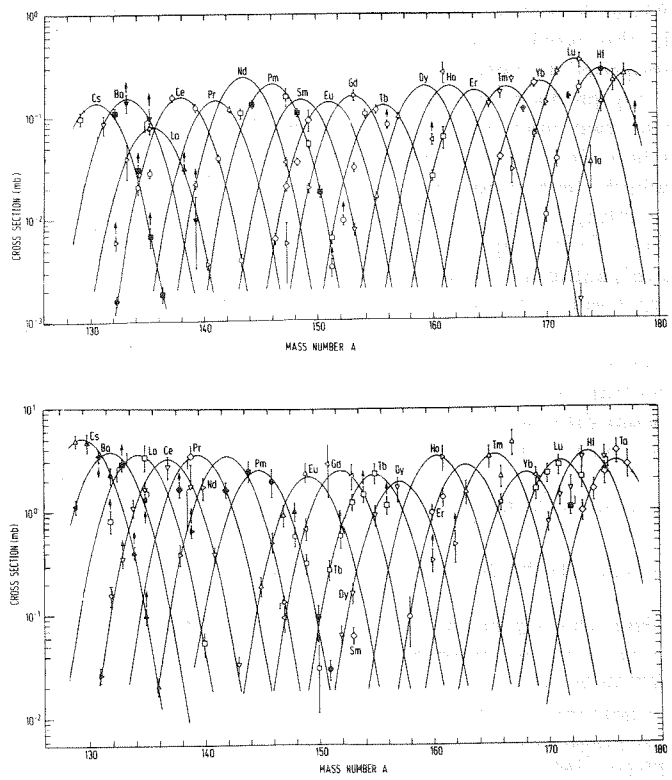

Fig. 1: Z,A-distribution of the lanthanides produced in the reaction $^{51}V + ^{197}Au$ at the barrier ($E_{cm} \equiv B$) (upper part) and for the increased bombarding energy ($E_{cm} = B + 25$ MeV) (lower part)

Glass Adsorption Chemistry for Decay Studies of ^{263}Ha

K.E. Gregorich, D.C. Hoffman, S.A. Kreek, D.M. Lee, B. Kadkhodayan, C.D. Kacher, M.R. Lane, E. Sylwester, M.P. Neu, N.J. Hannink
Lawrence Berkeley Laboratory, Berkeley, California
M. Schädel
GSI Darmstadt
J.V. Kratz
Institut für Kernchemie, Universität Mainz

The first chemical studies of element 105, Ha, in aqueous solution investigated the adsorption behaviour of tetra- and pentavalent ions from mineral acids on glass[1]. In these experiments, Gregorich and coworkers found that the group 5 elements Nb, Ta and Ha adsorb on the glass much better from strong nitric acid than do the group 4 elements. This separation procedure has in earlier experiments been used to make short-lived niobium isotopes from fission product mixtures accessible for γ−spectroscopy[2,3]. This procedure has the merits that it is fast, easy, clean, and reproducible enough to carry out many repetitive experiments by hand if no automated rapid chemistry apparatus like ARCA II [4] is available.

In a series of experiments to further investigate the decay properties of the new isotope ^{263}Ha[5,6] we again have applied the glass adsorption separation procedure to products formed in the ^{18}O + ^{249}Bk reaction at 93 MeV projectile energy in the target. It is expected from fusion-evaporation calculations with the code HIVAP that the excitation function for the 4n-channel peaks at this energy. The experiment, performed at the 88-inch cyclotron in Berkeley, was carried out in a way similar to that described in Ref. 1.

The activities recoiling out of the target were transported by a gas-jet to the fume hood where they were collected on a miroscope cover-glass. At the end of the 60-s collection time, the glass plate was removed from the collection site and placed on a hot plate. The potassium chloride aerosol spot on the glass plate was fumed with 3 μl of 15 M nitric acid. After this nitric acid dried, a second fuming was performed with 5 μl of 15 M nitric acid. When the second drop of nitric acid had dried, the nitric acid and the activities on the glass plate were removed by washing the plate with 1.5 M nitric acid. Any remaining acid was removed by washing the glass plate with acetone. The glass plate was immediately dried on the hot plate, cooled with a stream of air and placed onto one of eight PIPS-detectors. The detector efficiency was 35 % for α decay. The average time from the end of accumulation of the aerosols to the beginning of counting for α and SF decay was 56 s, and the counting time for each sample was 7 min.

In 1619 adsorption experiments we observed a total of 22 single fission fragments and 7 α's in an energy window between 8.30 and 8.69 MeV. From previous experiments [5,6] it is known that the α's of ^{262,263}Ha and ^{258,259}Lr are in this energy window. At 93 MeV bombarding energy the α's of the ^{263}Ha - ^{259}Lr pair are prevailing; these we expect to be in the energy window between 8.30 and 8.50 MeV.

Five of the observed seven α's appeared in this energy window, and we assign these to the pair ^{263}Ha - ^{259}Lr. The following α energies, given in MeV, were detected (event time in s after begin of counting): 8.331 (11), 8.389 (66), 8.438 (20), 8.445 (30), 8.455 (25), 8.560 (79), and 8.654 (4). A maximum likelihood analysis[7] of the time intervals, excluding the α's at 8.560 and 8.654 MeV, gives a half-life of 24 s with an upper limit (68% confidence limit) of 54 s and a lower limit of 14 s. A similar half-life analysis of the fission data gives 39 s (upper limit: 48 s, lower limit: 32 s). These results are in good agreement with the half-life of 27^{+10}_{-7} s reported in Ref. 5,6.

No time correlated $\alpha - \alpha$ pair for a ^{263}Ha - ^{259}Lr mother - daughter decay was observed. Therefore, the genetic link which would prove the assignment of the previously [5,6] and presently observed α's at 8.35 MeV to ^{263}Ha is still missing.

To our surprise, we observed two α-SF correlations. The α energies were 8.445 and 8.455 MeV and the time interval between the α and SF event was 7 s for each event. As it is known that the ^{263}Ha daughter ^{259}Lr, $T_{1/2}$ = 6 s, has a 20 % fission branch [8], the observation of an α - SF correlation is not surprising in itself but it clearly shows that the α's at about 8.45 MeV do not only belong to ^{259}Lr as assumed in the evalution of earlier data [5,6], but also originate from ^{263}Ha. Thus, the α-spectrum of ^{263}Ha is complex and overlaps, at 8.45 MeV, with the α-spectrum of its daughter, ^{259}Lr.

Adding our new data to the ones from a previous experiment the α to SF ratio for ^{263}Ha has slightly changed. Our presently best value for the fission branch is 68±9% compared to a value of 57^{+13}_{-15}% determined in the previous experiment [5,6].

References

[1] K.E. Gregorich et al., Radiochim. Acta 43, 223 (1988)

[2] H. Ahrens et al., Phys. Rev. C14, 211 (1976)

[3] M. Weis et al., J. Inorg. Nucl. Chem. 43, 437 (1981)

[4] M. Schädel et al., Radiochim. Acta 48, 171 (1989)

[5] J.V. Kratz et al., Phys. Rev. C45, 1064 (1992)

[6] M. Schädel et al., Radiochim. Acta 57, 85 (1992)

[7] K.E. Gregorich, Nucl. Instr. Meth. A302, 135 (1991)

[8] K.E. Gregorich et al., Phys. Rev. C45, 1058 (1992), and private communication about an improved value of 20 % for the ^{259}Lr fission branch from a recent experiment.

Status of the Λ–Hypernuclei Experiment at SIS

M. Schädel, W. Brüchle, E. Jäger, T. Krogulski, S. Polikanov, E. Schimpf, G. Wirth
GSI Darmstadt
Th. Aumann, J.V. Kratz, E. Stiel, N. Trautmann
Institut für Kernchemie, Universität Mainz

An experiment has been set-up and tested at SIS to study lambda-hypernuclei production in nucleus-nucleus collisions at and below the threshold energy by means of detecting in flight the delayed decay of hypernuclei with a lifetime of 100 - 200 ps.

The geometrical arrangement of the six low-pressure MWPC's, one START and two STOP counters on either side of the beam axis, together with the positioning of our stack of targets to apply the recoil distance technique which allows to detect delayed decays in flight, was described earlier [1]. The performance of our detection system, as obtained from measurements with a ^{252}Cf-source [2], was quite satisfactory. The known dimensions of the ^{252}Cf-source were reproduced by the measured distributions of fission fragment vertices and the bi-dimensional distribution of TOF versus dE/dx-signals represents the known distributions for ^{252}Cf fission fragments [2].

The first on-line measurement as a test was performed with a beam of 1.7 GeV/nucleon ^{20}Ne passing a stack of six Bi-targets, each one 150 μg/cm^2 thick and 2 · 10 mm^2 large, deposited on 6.7 mg/cm^2 thick Ti-backings. It was found that, at the presently available intensities of Ne-ions, the observed rate of prompt fission events did not cause any problems in the performance of our detection system to measure single and coincident fragments, and the track reconstruction technique could be applied to all detected events.

The resulting position distribution of *single* fragment hit points along the beam axis is shown in Fig. 1 (in the evalution each of the target plane positions was normalized to z=0).

The target plane separating the foreward and backward hemisphere is clearly visible in Fig. 1. To our knowledge, this is the first time that the recoil distance technique was successfully applied to a multi-target arrangement. The events in the shadow area are most likely not only due to delayed fission. Some may, for example be due to a not perfectly flat surface.

As an additional filter for good events, a *coincidence* between two fission fragments is required, and the resulting fragment distribution is shown in Fig. 2. The position distribution along the beam axis for prompt fission events (open area) was compared with that in a Monte Carlo simulation as developed for studies of hypernuclei produced in $\bar{p}$ annihilation reactions [3–5]. The momentum distribution of heavy recoil nuclei was approximated by $N(P_{||}) = N_0 \cdot (P_{||}/P_0) \cdot exp(-P_{||}/P_0)$ with P_0=425 MeV/c and a cut-off in the parallel momentum distribution at 1800 MeV/c. The calculated, dashed curve in Fig. 2 nicely reproduces the experimental data. The chosen P_0-value is in good agreement with the results from our detailed studies of prompt fission [6].

The vast majority of events displayed in Fig. 2 are coincidences between both fragments observed in the open area. After introducing the additional condition that one fragment is recorded in the *shadow* area, about 20 events are left. Their position distribution is shown in Fig. 3 together with a MC simulation of the delayed hypernuclei fission with a lifetime from [3]. These measurements thus comprise a successful test of our set-up to search for Λ–hypernuclei. We consider about 20 events observed in the shadow region as an indication of delayed fission in the reaction studied.

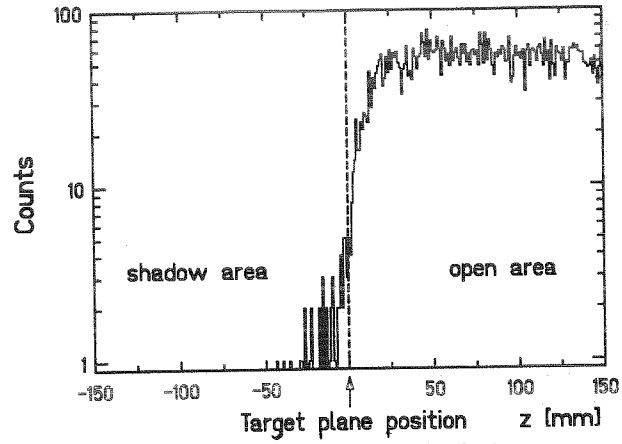

Figure 1: Single fragment position distribution.

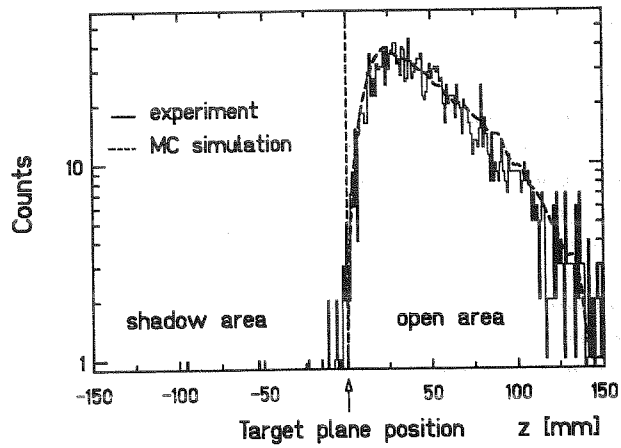

Figure 2: Position distribution of coincident fragments.

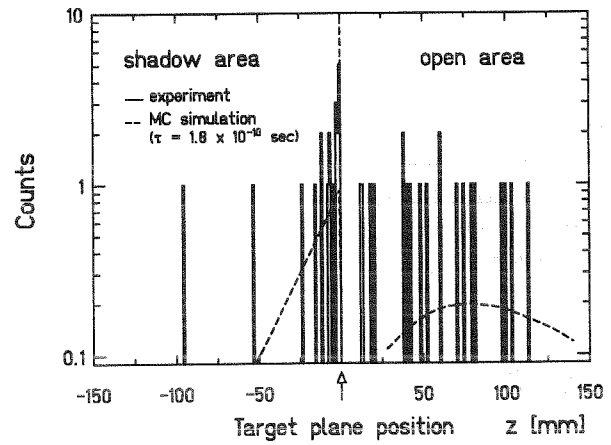

Figure 3: Distribution of coincident fragments with one fragment in the shadow area.

References

[1] E. Stiel et al., GSI Scientific Report 1990, GSI 91-1 (1991) p.323
[2] T. Krogulski et al., ibid p.322
[3] J. P. Bocquet et al., Phys. Lett. B182 (1986) 146
[4] J. P. Bocquet et al., Phys. Lett. B192 (1987) 313
[5] T.A. Armstrong et al., Preprint CERN-PPE/92-106 (1992)
[6] T. Krogulski et al., contribution to this report

Momentum Transfer in RHI Reactions Observed in the Fission Channel

T. Krogulski, W. Brüchle, S. Polikanov, M. Schädel, G. Wirth
GSI Darmstadt
E. Stiel, Th. Aumann, J.V. Kratz, N. Trautmann
Institut für Kernchemie, Universität Mainz

Momentum transfer in the reaction of 100, 500 and 1000 MeV/u ^{208}Pb with ^{209}Bi and ^{238}U targets was measured in the fission channel. For this purpose we have slightly modified the existing experimental set-up designed to study Λ-hypernuclei[1,2] changing only the targets.

Bi and U, 580 $\mu g/cm^2$ and 400 $\mu g/cm^2$ thick, respectively, was deposited on 40 $\mu g/cm^2$ C-backings, and these targets were inclined against the beam axis by 7°. This increased the effective thickness by a factor of 8 while the targets as seen by the MWPC's detecting fission fragments, were thin enough to measure coincident fission fragments.

From the reconstruction of fission fragment trajectories (measured angles and velocities) on an event-by-event basis we got the velocity components of the recoil nuclei parallel and perpendicular to the beam direction. Momenta can be calculated unequivocally if, in addition, energies of the fission fragments are measured. Since the kinetic energies were not measured in our experiment we mainly discuss the following observables: (i) the mean values of the parallel, $p_{||}$, and perpendicular, $p_\perp$, momentum components, and (ii) the dispersion of the $p_{||}$ – distribution. The mean values of velocities and momenta *per nucleon* are strictly identical for any mass distribution which is symmetric with respect to the average mass value. The dispersion of the velocities and momenta per nucleon of these distributions may differ somehow. However, it was checked that this effect is of second order by varying the initial mass of the fissioning system in a wide range.

From the experimental data, as summarized in Table 1, and compared with data from other experiments in Fig. 1, the following can be observed:

(i) $p_{||}$ is decreasing rapidly with increasing projectile energy, increasing projectile mass and increasing target mass,

(ii) $p_\perp$ depends weakly on the projectile energy, and it decreases along with the mass of the projectile,

(iii) in the fission channel induced by Pb-projectiles $p_\perp$ is much higher – 2 to 10 times – compared to $p_{||}$. At the same time the dispersion of the $p_{||}$ distribution is much lower – 4 to 14 times – than the mean value of $p_\perp$.

The first observation can be interpreted as an indication that the fission channel selects more and more peripheral reactions with increasing projectile energy. This effect has been observed earlier in reactions with lighter projectiles[4,5]. The observed target mass dependence has been discussed as a result of the increase of fissility[3].

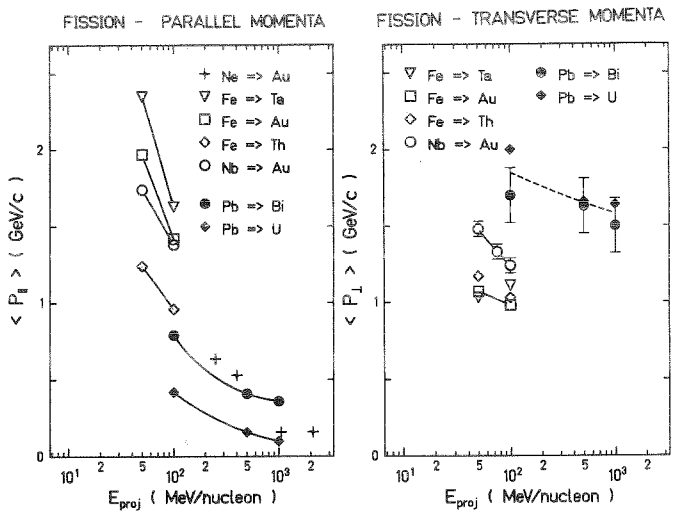

Figure 1: Mean parallel, $p_{||}$, and transverse, $p_\perp$, momentum of the fissioning system as a function of projectile energy. Data from this work, full symbols, are compared with data from Ref. 3,4, open symbols.

It is interesting to note that the observed mean values of the transverse momenta are very close to the calculated values for purely electromagnetic excitations. However, this can be accidental since the large widths of the observed $p_\perp$ distributions indicate strong nuclear contributions to $p_\perp$.

From the third observation we conclude that there can *not* be any *large isotropic* momentum contribution, e.g., from the deexcitation of an equilibrating hot system, on top of the parallel momentum distribution.This would give rise to a much larger dispersion of $p_{||}$, and one can conclude that the large transverse momentum, $p_\perp$, was transferred in the first stage of the reaction to the nascent, target-like fragment which then undergoes fission. This is clearly different from the picture which was developed for heavy fragments which do not fission[6].

References

[1] E. Stiel et al., GSI Scientific Report 1990, GSI 91-1 (1991) p.323
[2] M. Schädel et al., contribution to this report
[3] M. Begemann-Blaich et al., Phys. Rev. C45, 677 (1992)
[4] A.I. Warwick et al., Phys. Rev. C27, 1803 (1983)
[5] W.G. Meyer et al., Phys. Rev. C22,179 (1980)
[6] D.J. Morrissey Phys. Rev. C39, 460 (1989)

Table 1: Measured mean values of parallel, $< p_{||} >$, and transverse, $< p_\perp >$, momenta per nucleon from coincident target-like fission fragments. $\sigma(p_{||})$ is the dispersion of the parallel momentum distribution, and $< \Theta >$ is the folding angle. (The dispersion in $p_\perp$, not listed in Table 1, is similar to the ones observed in[3]) The values in brackets are momenta for the fissioning system assuming fragment masses of A=190 for Bi and A=220 for U targets. The estimated systematic errors are ± 0.5 GeV/c for $< p_{||} >$, ± 0.8 GeV/c for $< p_\perp >$, and ± 0.5° for $< \Theta >$.

Target	100 MeV/u				500 MeV/u				1000 MeV/u			
	< p|| > [MeV/c•u]	σ(p||) [MeV/c•u]	< p⊥ > [MeV/c•u]	< Θ >	< p|| > [MeV/c•u]	σ(p||) [MeV/c•u]	< p⊥ > [MeV/c•u]	< Θ >	< p|| > [MeV/c•u]	σ(p||) [MeV/c•u]	< p⊥ > [MeV/c•u]	< Θ >
^{209}Bi	4.1 (0.79 GeV/c)	1.9	8.9 (1.7 GeV/c)	150.4 °	2.2 (0.41 GeV/c)	0.58	8.6 (1.63 GeV/c)	154.7 °	1.9 (0.36 GeV/c)	0.59	7.9 (1.5 GeV/c)	157.8 °
^{238}U	1.9 (0.42 GeV/c)	1.7	9.2 (2.0 GeV/c)	153.5 °	0.72 (0.16 GeV/c)	0.85	7.6 (1.66 GeV/c)	164 °	0.48 (0.1 GeV/c)	0.80	7.5 (1.64 GeV/c)	167 °

Evidence for the excitation of the two-phonon giant dipole resonance in ^{197}Au

T. Aumann[1], W. Brüchle[2], M. Fauerbach[3], J.V. Kratz[1], M. Schädel[2], E. Stiel[1], K. Sümmerer[2], G. Wirth[2]
[1]Inst. f. Kernchemie, Uni Mainz, [2]GSI, Darmstadt, [3]Inst. f. Kernphysik, TH Darmstadt

Very large cross sections were measured by an activation method in relativistic heavy ion collisions at SIS energies for the 1n removal from ^{197}Au - targets [1, 2], which are for heavy projectiles dominated by the electromagnetic excitation of the giant dipole resonance (GDR). Due to high excitation probabilities also multiple excitations of the GDR should become important [3]. Since higher-order GDR excitations are expected to contribute mainly to the emission of more than one neutron, we have measured the 2n cross section for 1 GeV/nucleon ^{197}Au + ^{197}Au, and 3n cross sections for 1.7 GeV/nucleon ^{20}Ne, 1 GeV/nucleon ^{86}Kr, ^{197}Au, and ^{209}Bi + ^{197}Au. The procedure of cross section determination is described in detail in Ref.[2].

For the lighter projectiles Ne and Kr the resulting 3n-out cross sections are only insignificantly larger than the nuclear contribution estimated with the intranuclear cascade model ISABEL. If the small predicted contribution from electromagnetic dissociation (ED) (2.0 mb and 16 mb, respectively) is added to the calculated INC values, excellent agreement with the measured total cross sections is obtained, which give confidence in the calculated nuclear cross sections.

For the heavier projectiles, where multi-photon absorption can occur, the experimental ED cross sections are shown in Fig.1 compared to Weizsäcker-Williams (WW) calculations. The solid line represents a simple WW calculation including single-phonon GDR as well as isoscalar and isovector giant quadrupole (GQR) excitation. For the 1n channel the data are systematically overestimated by the WW calculation as noted earlier [1, 2], while for the 2n and 3n cross sections, the situation is reversed. For Au and Bi projectiles, the experimental 3n cross sections exceed the simple WW prediction by a factor 5.7 and 6.8, respectively. These dramatic deviations can be explained by the excitation of the double GDR: The dashed line in Fig.1 was obtained from a modified WW calculation taking into account multi-phonon excitation following the approach of Llope and Braun-Munzinger [4]. This results in a lowering of the calculated 1n-out cross sections (because only first order contributes), and in increasing the 2n and 3n cross sections, as demanded by the data. Fig.1 shows,

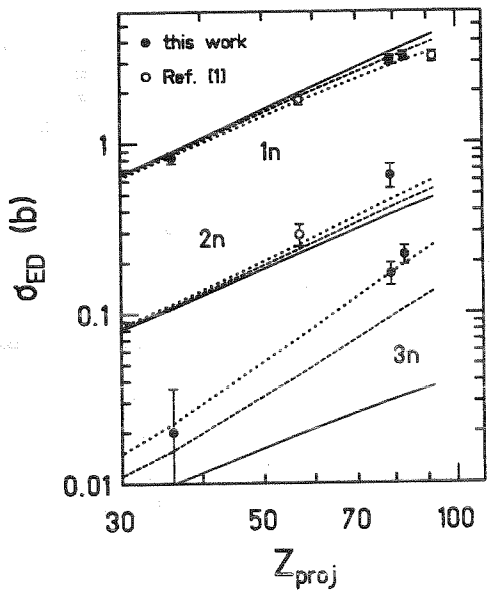

Fig.1. ED cross sections for 1n-, 2n-, and 3n-removal from a ^{197}Au target as a function of projectile charge. All experimental data points are scaled to the same bombarding energy of 1 GeV/nucleon. The curves represent WW calculations (see text).

that especially the magnitude of the 3n ED cross section is a sensitive measure of the strength of higher-order GDR excitations. The remaining deviations can be attributed to an enhancement of the double GDR excitation strength compared to the harmonic oscillator model underlying our calculations. Such an enhancement was recently measured in ^{136}Xe projectiles by the LAND group [5]. The dotted line in Fig.1 is obtained if the probability for the two-phonon excitation of the GDR is increased by a factor of 2.2, which minimizes the rms deviation for all three channels.

Another important input parameter for the WW calculation is the minimum impact parameter, b_{min}, below which nuclear processes dominate. In Fig.2, the influence of b_{min} on the calculated cross sections is shown. The dashed line is the same as in Fig.1 (including multi-phonon excitation, without enhancement), using a parametrization of b_{min} given by Kox et al. [6], which is for the heavy systems equivalent to $b_{min} \approx 1.4(A_p^{1/3} + A_t^{1/3})$fm. This choice of b_{min} gives the best reproduction of the 1n cross sections, which are measured with the highest precision. The BCV parametrization as used in [1, 2], corresponding for the heavy projectiles to $b_{min} \approx 1.3(A_p^{1/3} + A_t^{1/3})$fm, gives even larger cross sections (dotted line in Fig.2). In this case an enhancement factor of 1.9 for the double GDR is needed to remove the remaining deviations, which is similar to the value obtained for the Kox parametrization. Finally there is a calculation shown as the solid curve with a cut-off radius $b_{min} = 1.2(A_p^{1/3} + A_t^{1/3})$fm, as used in Ref.[3, 4]. This parametrization gives very good agreement for the 2n and 3n channels but grossly overestimates the majority of the 1n cross sections. For this parametrization it is not possible to reproduce all three channels simultaneously by introducing an enhancement factor.

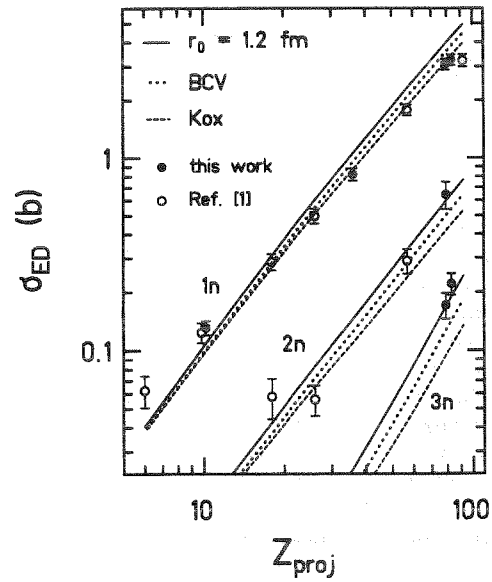

Fig.2. Same as Fig.1, but the curves represent WW calculations with different parametrizations for the cut-off parameter.

References

[1] J.C. Hill *et al.*, Phys.Lett.B273(1991)371, and refs. therein.
[2] T. Aumann *et al.*, GSI-Preprint, GSI-92-47 (1992).
[3] C.A. Bertulani and G. Baur, Phys. Rep. 163 (1988) 299.
[4] W.J. Llope *et al.*, Phys. Rev. C 41 (1990) 2644.
[5] LAND Collaboration, GSI-Preprint GSI-92-64 (1992).
[6] S. Kox *et al.* Phys. Rev. C 35, 1678 (1987).

A Low Temperature Irradiation Facility at the UNILAC Beamline X1

J. Wiesner [1], G. Wirth [2], H. Fueß [1], E. Jäger [2], E. Schimpf [2]

[1] TH Darmstadt, [2] GSI Darmstadt

A low temperature irradiation facility has been set up at the UNILAC beamline x1. The experimental arrangement was mainly designed for the investigation of heavy ion induced modifications of high T_c superconductors, but it may be used for other low temperature irradiations as well. During heavy ion irradiation the sample can be kept constant at any temperature between room temperature and 20K. Special attention was drawn to a reliable beam monitoring. The beam diagnostics allows to guarantee a homogenity of the heavy ion beam spot within ± 10% of the mean intensity over an area of at least 1.5x1.5 cm^2 and to determine the integrated ion flux on a sample with a precision of 10%. The resistive transition R(T) and the critical current density J_c of high T_c superconducting samples can be measured in situ. While keeping a sample on the preset temperature it can be moved from the target position for heavy ion irradiation into a shielded position between the poles of a 1.1 T normal conducting electromagnet for the measurement of magnetic field dependent quantities as R(T,B), J_c(B) and Hall effect.

For cooling, the sample is mounted on the cold head of a double stage cryogenic refrigerator (Leybold RGD210) operated in a closed gas cycle. The temperature is adjusted by a resistive heater fitted to the 2nd stage and controlled by a temperature controller (LakeShore DRC91CA). Two silicon diode temperature sensors (LakeShore DT470) are mounted at the 2nd stage and on the sample holder.

Irradiation of the samples is performed in a defocused beam mode without wobbling or scanning the beam over the target. Tuning of the beam to get a homogenous beam profile covering the whole sample is done in a first step with the aid of various luminiscence screens of different sensitivity. To determine the absolute beam intensity, ions passing a circular aperture of 100 μm or 200 μm in diameter are counted by a scintillator NE102A coupled to a photomultiplier tube. For beam profiling the aperture is mounted on a motorized high precision x-y translation drive. Varying beam intensities while scanning the beam profile are taken into account by a reference signal from a secondary electron transmission detector SEETRAM. Typical beam intensities for high T_c superconductor irradiation experiments are 10^8 ions/cm^2s (≃0.02 pnA) with an integral fluence per sample of 10^{10} - 10^{12} ions/cm^2. In the beam profile scanning mode ion counting of only a few macropulses per scan position is sufficient and radiation damage of the scintillator material is no problem. The selection of single macropulses under experiment control is done with the fast UNILAC chopper. For the integral fluence counting the scintillator is moved automatically stepwise behind the fixed aperture after a preset number of heavy ion hits was registered. The beam monitoring can be checked at any time by introducing a standard glass target with subsequent etching and track counting.

The resistive transition R(T) and critical current density J_c of the samples are measured using a programmable current source (Keithley 220) and nanovoltmeter (Keithley 182). The measurements are performed in four point geometry with alternating dc-current direction. All instruments of the experimental setup are connected to an IBM PC via IEEE-bus under the control of special software. The complete setup was successfully tested. First results were obtained with ^{197}Au ions of 13.3 MeV/u on structured epitaxial thin $YBa_2Cu_3O_{7-x}$ films of 200nm thickness prepared by CVD at the Hoechst AG. As an example fig.1 shows the dependence of J_c at 85K on the heavy ion fluence at various external magnetic fields.

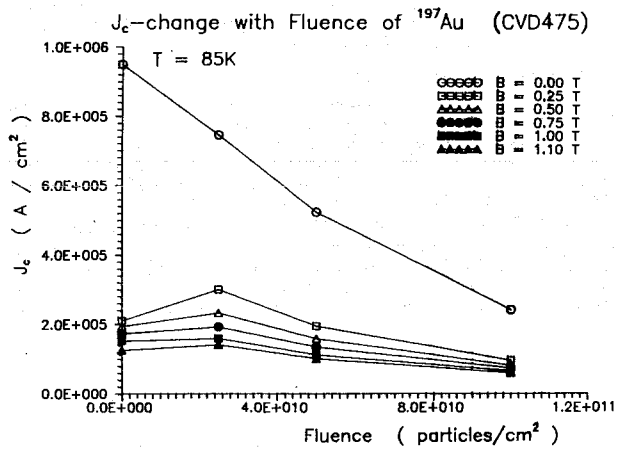

Fig.1 J_c versus the fluence of 13.3 MeV/u^{197}Au ions. All data were taken with the same YBCO sample. The external magnetic field was oriented parallel to the c-axis of the epitaxial film.

A TBP Extraction Procedure to Separate Elements 104 and 105

K.E. Gregorich, D.C. Hoffman, S.A. Kreek, D.M. Lee, B. Kadkhodayan, C.D. Kacher, M.R. Lane, E. Sylwester, M.P. Neu, N.J. Hannink
Lawrence Berkeley Laboratory, Berkeley, California
M. Schädel
GSI Darmstadt
J.V. Kratz
Institut für Kernchemie, Universität Mainz

For a detailed investigation of the decay properties of the most neutron-rich, heavy element isotopes chemical separations preceeding the nuclear decay measurements are quite often a necessary prerequisite. For example, the isotope ^{263}Ha produced in the ^{249}Bk(^{18}O,4n) reaction was first identified after a chemical separation of an element 105, Ha, fraction [1], or the isotope ^{262}No was found as the EC decay product of ^{262}Lr in a measurement of a chemically separated Lr fraction [2]. The chemical technique has to be fast enough to cope with the half-life. Sometimes even isotopes with half-lives as short as 5 ms, e.g. ^{262}No, can be investigated in a chemically purified sample of the precursor with a long enough half-life, e.g. the 216 min ^{262}Lr, provided that an adequate measuring technique is available [2].

We have developed and tested a separation to search for a possibly existing EC branch in the new isotope ^{263}Ha, $T_{1/2}$ = 27 s. The observed spontaneous fission branch (about 60 %) of this isotope may not originate from the fission of the Ha isotope but rather from the spontaneous fission (SF) of the EC decay daughter ^{263}Rf, a presently unknown nucleus. If the ^{263}Rf half-life is about 20 s or longer, which from the presently known SF half-life systematics can not be excluded, a fast chemical separation of the ^{263}Rf daughter from ^{263}Ha followed by a SF measurement of the Rf fraction would prove the existence of an EC branch in ^{263}Ha. In addition, it would give important information about a new isotope, and it would open the path to study the fission properties of this isotope.

In order to avoid two time consuming extraction and back extraction steps in the separation of tetra- and pentavalent ions we selected the liquid-liquid extraction system tri-n-butyl phosphate, TBP, in benzene as an organic and 10 M nitric acid as the aqueous phase. This extraction system has the advantage that the tetra- and pentavalent ions are separated with high yield and a good decontamination from the actinides. From the extraction behaviour of tetravalent ^{95}Zr and pentavalent ^{95}Nb [3] one expects that Rf^{4+} extracts into the organic phase while Ha^{5+} remains in the aqueous phase. As the organic phase can be evaporated to dryness much faster than the aqueous phase only a short time of about 20 s is needed to begin the measurement of a Rf fraction after the separation from Ha.

We have applied the TBP extraction procedure to products formed in the ^{18}O on ^{249}Bk reaction at 93 MeV projectile energy in the target at the 88-inch cyclotron in Berkeley. Fusion-evaporation calculations predict the maximum cross section for the ^{263}Ha production at this energy.

The activities recoiling out of the target were transported by a gas-jet to the fume hood where the activity bearing aerosols were collected on a Teflon plate. At the end of the 60-s collection time, this plate was removed from the collection site. The potassium chloride aerosol spot on the plate was dissolved in 15 μl of 10 M nitric acid. This solution was added to 30 μl of 0.25 M TBP in benzene in a 1 ml centrifuge cone and mixed in an ultrasonic bath for 5 seconds. The phases were separated by centrifuging for about 5 seconds. The organic phase was removed and placed on a glass cover slip on a hot plate evaporating the organic phase, leaving the ^{263}Rf on the cover slip. The slip was placed onto one of eight PIPS-detectors. The detector efficiency was 35 % for α decay. The average time from the end of accumulation of the aerosols to the beginning of counting for α and SF decay was 56 s, and the counting time for each sample was 7 min.

In 321 extraction experiments we did not observe a single fission event which would have indicated an EC branch in ^{263}Ha. Here we have to keep in mind that we are only sensitive to observe this branch if the half-life of ^{263}Rf is longer than about 10 s. Also, as expected, no α events from ^{263}Ha in the energy window between 8.30 and 8.50 MeV were observed. As the α-spectrum was very clean and a complete separation from possibly interfering actinide activities was achieved, the TBP extraction system has in this test been proven to be an adequate system to search for ^{263}Rf as a possibly existing, longer-lived EC decay daughter of ^{263}Ha. From a preceeding experiment in which the nuclear decay of ^{263}Ha has further been investigated [4] under experimental conditions which were similar to the ones described in this contribution except for the chemical separation part itself, we can estimate that a maximum of about four SF events would have been expected in case that all fission events observed in the ^{263}Ha decay originate from an EC branch. At the moment the number of experiments is still too low to draw any conclusion, and a continuation of these experiments is needed.

To test the quality of this separation procedure for Rf and to determine an exact chemical yield for Rf in this separation one needs to produce the known isotope ^{261}Rf in the ^{248}Cm(^{18}O,5n) reaction. Because of beam time limitations we were only able to perform 103 extractions with reaction products formed in the reaction with ^{248}Cm. No α events from ^{261}Rf in the energy window between 8.10 and 8.40 MeV were observed. Taking a cross section of 5 nb [5] and appropriate efficiencies into account one would expect to detect about three αs. Again the α-spectrum was very clean and a complete separation from actinides was achieved in this TBP extraction. A larger number of experiments has to be carried out to measure the chemical yield of the Rf extraction into TBP from 10 M nitric acid before a new series of experiments with ^{249}Bk shall be started.

References

[1] J.V. Kratz et al., Phys. Rev. C45, 1064 (1992)

[2] R.W. Lougheed et al., LLNL Nucl. Chem. Div. Annual Report88, UCAR 10062-88, p.135

[3] K.R. Czerwinski, Ph. D. Thesis, LBL-32233 (1992)

[4] K.E. Gregorich et al., contribution to this report

[5] A. Ghiorso et al., Phys. Letters 32B, 95 (1970)

The Lawrencium Fraction - a Potentially Useful By-Product of Ha Experiments

H.U. Becker, J.V. Kratz
Institut für Kernchemie, Universität Mainz

B. Schausten, W. Brüchle, M. Schädel
GSI, Darmstadt

We have developed a chemical separation to get access to a Lr fraction for nuclear decay studies as a by-product from our investigation of element 105. At 99 MeV bombarding energy, which is the optimum for the ^{249}Bk (^{18}O,5n) ^{262}Ha channel, ^{260}Lr is produced in the (α,3n) reaction with a cross section of 8.3 $\pm$ 1.7 nb [1].

The motivation for more detailed studies of the decay of ^{260}Lr, presently known as an α-emitter with 3 min half-life (E_α = 8.03 MeV) [2], is the search for a possible EC-branch in the decay of ^{260}Lr. An EC decay would open the path to study the SF decay of ^{260}No, currently believed to decay with a half-life of 100 ms by spontaneous fission (SF) [3]. The measurement of time intervals between ^{260}No fission fragments and preceeding characteristic No K X-rays from the ^{260}Lr EC decay, with a set-up and technique similar to the ones used in the discovery of ^{262}No [4] or the study of EC-delayed fission of ^{234}Am [5], would allow to verify the assignment [3] of the 100 ms fission activity to ^{260}No. The counting equipment is discussed in a companion contribution to this report [6]. To reduce the background of γ-radiation in the No K X-ray windows, e.g. from fission products or reaction products from projectile interactions with the target backing which would lead to too many random events [6], and to separate ^{260}Lr from Fm and Md, a specific Lr chemistry is required.

The procedure is based on previous work [2] in which we determined the elution position of Lr relative to the heavier lanthanides in column chromatographic experiments with buffered α-hydroxiisobutyric acid (α-HIB) as an eluent and the strong cation exchange resin Aminex A6 (17.5 $\pm$ 2 μm) as the stationary phase. Previously [2], larger columns of 2 mm · 60 mm were used as compared to the (1.6mm · 8mm) columns of ARCA II currently used in our Ha studies. With the half-life of ^{260}Lr being 3 min compared to the 0.5 min of ^{262}Ha it is desirable to repete several collection and elution cycles for ^{262}Ha with typical cycle times of 60 s before eluting ^{260}Lr from the same column. Immediately the following important question arose: how often can we collect and elute a Ha fraction before any actinide activity breaks through, what is the best concentration and pH to first elute Ha followed by a Lr elution, and what fraction shall be eluted for the Lr fraction that is clean enough (no fission products) for X-ray-SF correlation measurements.

To this end, radioactive tracers of Lu, Ho and Sm were used, and various α-HIB concentrations were tested. Lr is known to be eluted slightly ahead of the Ho position [2].

With unbuffered 0.05 M α-HIB, which elutes Ha in 50 μl [7], we observed no elution of Lu below 250 μl. The elution starts after about 250 μl and it reaches an elution of 44% after 500 μl. The elution of Ho begins after 500 μl. Sm is not eluted even in 3 ml 0.05 M α-HIB.

Good separations of Lu and Ho can subsequently be achieved with α-HIB concentrations of 0.1 M at pH 4.85, but the elution of Ho is too slow and the expected elution of Lr is not fast enough for our separations. After the raising of the α-HIB concentration to 0.12 M at pH=4.85 we observed a much faster elution of Ho. At higher concentrations of α-HIB we can not guarantee the separation from the other actinides.

The elution of Lu, Ho and Sm in 0.12 M α-HIB at pH=4.85 is shown in Fig.1. The elution of Ho is complete within 200 μl. Thereafter the elution of Sm sets in.

For the elution of Lr, a small volume and a short elution time are required. From Fig.1 we conclude that >90 % of Lr can be eluted in 100 μl of 0.12 M α-HIB at pH=4.85. In the Ha experiments, in which Ha is eluted in 50 μl [7] of unbuffered 0.05 M α-HIB, Lr will not be eluted before about 350 μl. Therefore, we can safely perform three subsequent Ha elutions with the necessary washing procedures on the same column, and then elute the Lr.

Thus, the cycle of experiments to be performed on a given cation exchange column in ARCA II will be as follows: There will be three subsequent one-minute collections of activity followed in each case by the dissolving of the activity in 0.05 M α-HIB, and the elution of a Ha fraction (for further studies of the decay of 27-s ^{263}Ha). Then, the 3-min ^{260}Lr collected on the column is eluted in 0.12 M α-HIB at pH=4.85, and is assayed for No K X-rays and ^{260}No fissions.

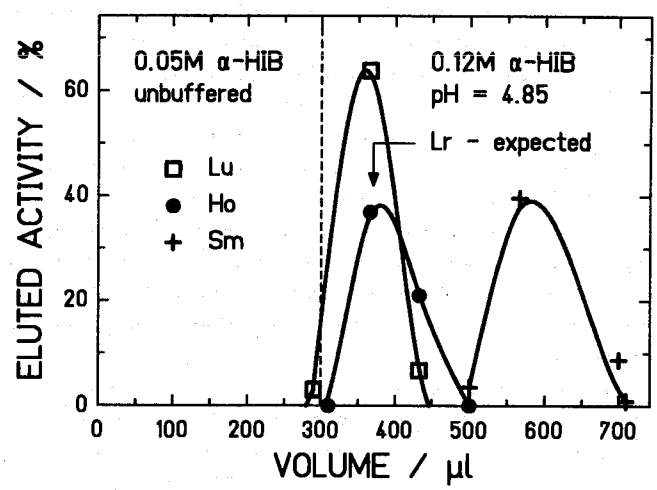

Fig. 1: Separation of Lu, Ho and Sm in ARCA II on a 1.6mm · 8mm column containing Aminex A6 with 0.12 M α-HIB, pH=4.85

[1] D. C. Hoffman et al. J. Radioanal. Nucl. Chem. 124, 135 (1988)
[2] W. Brüchle et al., Inorg. Chim. Acta 146, 267 (1988)
[3] L. P. Somerville et al., Phys. Rev. C31, 1801 (1985)
[4] R. W. Lougheed et al., Report UCAR 10062-88, 135 (1988)
[5] H. L. Hall et al., Phys. Rev. C41, 618 (1990)
[6] W. Brüchle et al., contribution to this report
[7] M. Schädel et al., Radiochim. Acta 57, 85 (1992)

A Test Experiment to Search for Electron Capture Decay of ^{262}Ha

W. Brüchle, E.A. Jäger, M. Schädel, B. Schausten, E. Schimpf
GSI Darmstadt
H.U. Becker, J.V. Kratz, H.P. Zimmermann
Institut für Kernchemie, Universität Mainz
H. Gäggeler, D. Jost, D. Vermeulen
Paul Scherrer Institut, Villigen, Switzerland
K.E. Gregorich, D.C. Hoffman, B. Kadkhodayan, S. Kreek, D.M. Lee, A. Türler
Lawrence Berkeley Laboratory, Berkeley, California
P.A. Baisden
G.T. Seaborg Inst. for Transactinium Science, Livermore, California

During our studies of the decay of 34 s ^{262}Ha and 27 s ^{263}Ha [1-3], produced in the reactions ^{249}Bk(^{18}O,5n) and ^{249}Bk(^{18}O,4n), ^{262}Ha was detected by measuring the associated fission and α activities, and the α- decays of its daughter 4.3 s ^{258}Lr. ^{262}Ha decays predominantly (67%) by α- decay. Time correlated pairs of α- particles from mother and daughter decays confirmed this assignment. The fission branch may result from direct spontaneous fission (SF) of ^{262}Ha, or from the electron capture (EC) daughter $\approx$47ms ^{262}Rf, which decays by SF.

To detect a possible EC branch in the decay of ^{262}Ha we planned a correlation experiment in which K x-rays from EC decay shall be registered in listmode together with the subsequent SF energies and time informations. If the EC decay of ^{262}Ha exists, this could give valuable information about the decay properties of ^{262}Rf, as todays assignment originates only from cross bombardments and half- life systematics [4].

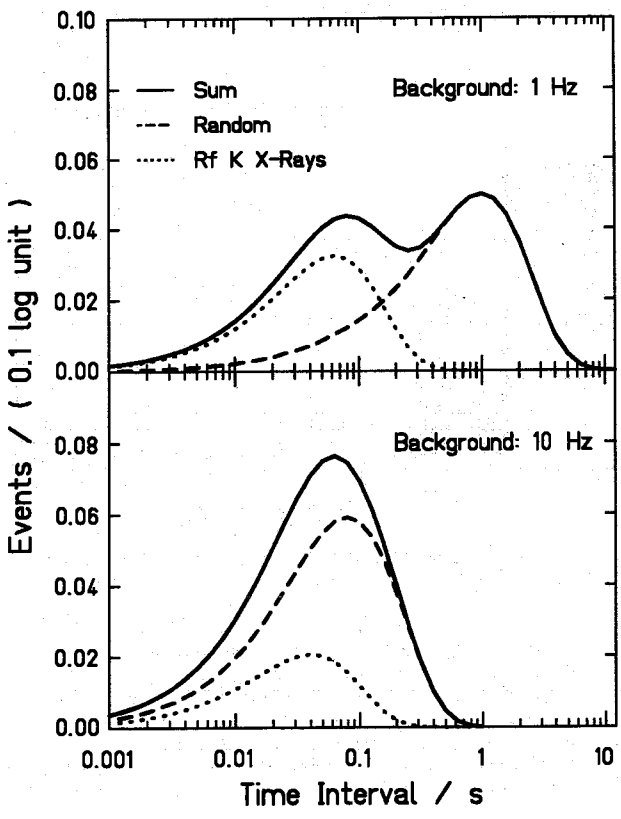

Fig.1: Calculated time distributions for a 47ms SF nuclide and 1Hz, resp. 10Hz background radiation in the Rf K x-ray region.

We tested a combination of the fast automated liquid chromatography system ARCAII [5] with a new measuring setup for time-correlation measurements. The time-correlation method for EC decay followed by SF decay was successfully applied [6,7] to identify 370μs ^{258}Fm and 5ms ^{262}No. The K x-ray signal from the EC decay, characteristic of the daughter element, starts a clock which is stopped when a fission fragment from the SF decay of the daughter nucleus is registered. We stored all x-rays in the region of interest and all fissions in listmode together with a clock information precise to 1μs. The following two experimental parameters are most important for a successful experiment: (i) the efficiency for the detection of fission fragments and especially K x-rays has to be as high as possible, and (ii) the stochastic background from γ-radiation of interfering reaction products or the natural background has to be reduced below a certain limit. Fig. 1 shows a simulated time distribution under the assumption of 41% detector efficiency, a half- life of 47ms, and random background of 1Hz. One clearly would be able to distinguish the decay of a 47ms nuclide from noise. The same simulation for 10Hz background shows that it would (at least within our statistics) not be possible to evaluate the desired data in that case.

To achieve a low background we choose a chemical separation with cation exchangers [2] performed with ARCAII. Trivalent actinides and rare earth elements and tetravalent elements like Zr and Rf were strongly retained on the columns, while pentavalent elements like Ha were eluted very fast. The samples were deposited on 0.15mm thick nickel foils; these samples were mounted in a distance of 3mm in front of a Si fission detector, and sandwiched between two HPGe detectors with 41% geometric efficiency each. The specially mounted Si detector (PIPS) with 450mm^2 active area yielded 37.5% α- efficiency (75% for SF). The α- and SF- spectra were very clean, but the contaminations in the Rf K x-ray windows by γ-radiation from fission products (Nb, Mo, Tc..) were so strong that the rate in the x-ray detectors was considerably higher than 10Hz.

1. J.V. Kratz et al., Radiochim. Acta 48, 121 (1989)
2. M. Schädel et al., Radiochim. Acta 57, 85 (1992)
3. J.V. Kratz et al., Phys. Rev. C45, 1064 (1992)
4. L.P. Somerville et al., Phys. Rev. C31, 1801 (1985)
5. M. Schädel et al., Radiochim. Acta 48, 171 (1989)
6. E.K. Hulet et al., Phys. Rev. C34, 1394 (1986)
7. R.W. Lougheed et al., LLNL Report UCAR 10062-88 (1988)

Fast Ha Separations with ARCA as a Test for the Chemical Separation of Element 106

W. Brüchle, K.H. Behr, E. Jäger, M. Schädel, B. Schausten, E. Schimpf
GSI Darmstadt
H.U. Becker, J.V. Kratz, A. Nähler, N. Trautmann, B. Wierczinski, H.P. Zimmermann, S. Zauner
Institut für Kernchemie, Universität Mainz
K.E. Gregorich, D.C. Hoffman, B. Kadkhodayan, S. Kreek, D.M. Lee, A. Türler
Lawrence Berkeley Laboratory, Berkeley, California

In a series of experiments to investigate further the chemical properties of element 105, Ha, and the decay characteristics of 34 s ^{262}Ha and 27 s ^{263}Ha [1], we have developed fast chemical separation procedures for Ha [2-4], which partly could also be used to separate element 106 from complex reaction product mixtures. For the production of an element 105 fraction, and to produce a characteristic spectrum of reaction products typical in heavy element research, we used the reactions ^{249}Bk(93MeV ^{18}O,4n)^{263}Ha and ^{249}Bk(99MeV ^{18}O,5n)^{262}Ha. Some of the previously used procedures like extraction into TIOA [2] or DIBC [4] are relatively slow because the activities are first extracted into the stationary organic phase and then in a second step backextracted and eluted. An additional disadvantage is the use of concentrated acids which tend to corrode our apparatus ARCAII [5], and are not so easily evaporated to prepare a sample for α-spectroscopy and spontaneous fission (SF) measurements. To overcome these disadvantages we have developed, tested, and partially applied two fast alternative separation procedures on a cation exchange resin [3,6]; one an elution with α-hydroxiisobutyric acid (α-HIB), and the other one with HCl- HF mixtures. These separations may in addition to Ha separations be well suited to perform chemical separations in experiments to search for new isotopes of element 106.

In our ^{18}O + ^{249}Bk test experiment the produced activities are transported on-line by a He/KCl- jet to the chemistry apparatus where the aerosols are collected on a frit. After 1 min collection time the activity was washed from the frit onto a microchromatography column (1.6mmx8mm) filled with a strongly acidic cation exchange resin (Aminex® A6, particle size 17.5 ± 2μm). With 5x10^{-2}m α-HIB as washing solution we were able to get high decontaminations from trivalent ions (actinides) and tetravalent ions (Zr, Hf, Rf) within 3 seconds [3]. After evaporation to dryness on a Ta disc and fuming off the α-HIB, alpha- particle and SF pulse- height analyses were performed using a system of 8 300mm^2 PIPS detectors. For mother-daughter correlations we stored all events with the GOOSY-system [7]. Independant monitor spectra were collected with a Canberra ND9900 system.

In a first block of experiments with α-HIB the Ha yield was lower than expected for reasons which remain unclear at the moment. To use a solvent which should be very well suited to dissolve our species we switched to 0.1M HCl/10^{-2}M HF as eluens. This system was tested before [6] with shortlived tungsten isotopes, but not with an actinide target. Po contaminations from reactions with small lead impurities in the target, and heavy actinide (Fm) transfer products, were so significant (Fig. 1) that we switched to 0.1M HCl/5x10^{-4}M HF as eluens. From our previous experiments [6] we know that the separation from impurities is much better at this lower HF concentration. Small contaminations could be assigned to Fm nuclides, which were at a level below 10^{-4} from the produced activities (Fig.2). This system seems promising with respect to velocity and decontamination. The α's which we still observe between 8.2 MeV and 8.7 MeV, an energy window in which we would search for characteristic α's of ^{265}106 in a ^{248}Cm(^{22}Ne,5n) reaction, can in this ^{18}O + ^{249}Bk reaction be attributed to ^{262,263}Ha and its daughter ^{258,259}Lr.

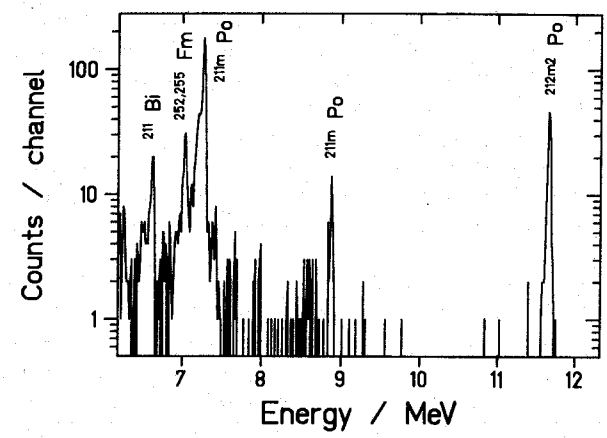

Fig.1: α-spectrum of a Ha fraction (as a test for element 106) eluted in 0.1M HCl/10^{-2}M HF

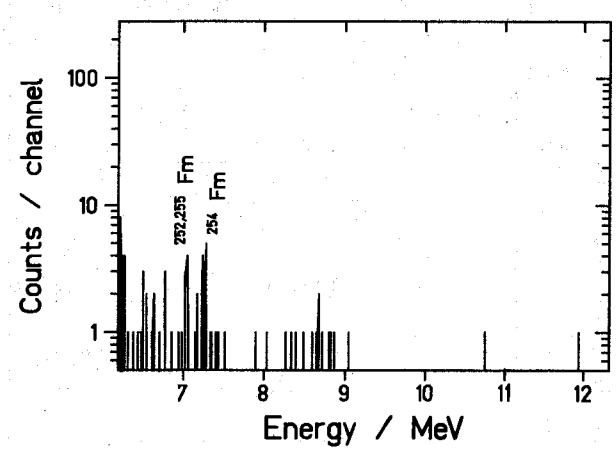

Fig.2: α-spectrum of a Ha fraction (as a test for element 106) eluted in 0.1M HCl/5x10^{-4}M HF

1. J.V. Kratz et al., Phys. Rev. C45, 1064 (1992)
2. J.V. Kratz et al., Radiochim. Acta 48, 121 (1989)
3. M. Schädel et al., Radiochim. Acta 57, 85 (1992)
4. M.K. Gober et al., Radiochim. Acta 57, 77 (1992)
5. M. Schädel et al., Radiochim. Acta 48, 171 (1989)
6. W. Brüchle et al., GSI Scientific Report 1991, GSI 92-1, p.315
7. H.G. Essel et al., GSI Scientific Report 1991, GSI 92-1, p.391

Characterisation of the Properties of the KCl-Aerosol Particles in a He-Gas Jet

R. Günther, A. Weber, J.V.Kratz,
Institut für Kernchemie, Universität Mainz
M. Schädel, E. Jäger, E. Schimpf
GSI Darmstadt

In heavy element chemistry research a He-gas jet is commonly used to transport the reaction products to the chemical apparatus. In recent experiments, large fluctuations in the transport efficiency were observed. The reasons for the malfunction of the jet are unknown and diagnosis is needed that determines the properties of the aerosol particles (KCl). The devices used for this purpose are a Differential Mobility Analyser (DMA) and a Condesation Nuclei Counter (CNC). This system can be used in two ways, as a generator of a monodisperse aerosol, or as an analyser of the size distribution of the particles.
The DMA is based on the relation between the electrical mobility Z_p of a singly charged particle and its diameter D_p.[1] In order to ensure a known amount of singly charged particles they pass through a bipolar charger (Kr-85). Through frequent collisions between the particles and the ions an equilibrium charge distribution given by Boltzmanns law is obtained. After charging, the aerosol is added to a clean gas and flows down an annular space between two cylindrical electrodes. The inner particle free core and the laminarity of the flows prevent particles from reaching the inner electrode by brownian motion. When a voltage is applied to the inner electrode the resulting electrical field causes the particles of opposite polarity to move towards the inner rod. By adjusting the voltage, it is possible to select particles of a certain mobility.

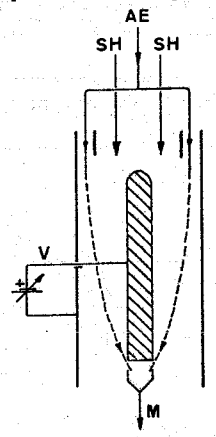

Figure 1: Schematic of the differential mobility analyser (DMA)[2]

After the separation of the DMA the monodisperse aerosol particles are fed into a Condensation Nuclei Counter (CNC). In the CNC the paricles act as condesation nuclei in the following heterogeneus condensation of n-Butanol on the particles. The droplets grow to about 10 μm independently of the initial particle size. Then the number concentration of these large particles can be detected by light scattering.
In experiments to investigate the chemical and nuclear properties of the heaviest elements after a transport in a KCl aerosol jet, the particles are generated by evaporation at about $670°C$ and condesation of KCl-salt in an oven at typical He-flow rates of about 1 - 3 lpm. Subsequently the size distribution changes because of coagulation and diffusion losses. A typical size distribution is given in Fig. 2.

According to the production conditions then geometrical mean diameter D_g ranges from $100nm$ to $250nm$. It was found that D_g increased with increasing temperature as attributed to an increase in mass production. As the flow rates increased, while all other parameter were kept constant, the geom. mean diameter first increased, reached a maximum, and then decreased. These results offer the possibility to adjust the size distribution by varying temperature and flow rate. The time-dependence of the size distribution was found to be small while the mass yield decreased with increasing time.
Next, the attachment to the aerosol particles of radioactive isotopes produced by fission of U-235 with reactor neutrons was studied by γ-spectoscopy. Fig. 3 shows the results.

In the case of diffusion-controlled attachment of isotopes on the particles the slope should be about 2 for particles of about $100nm$.[3] Our result disagrees with this prediction. This indicates that other processes than diffusion are involved in the deposition of the fission products on the particles.
Finally, the influence of radiation on carrier gas and aerosol particles was investigated. It was found that in particle free He no particles were produced in the target chamber by irradiation. On the other hand, for particle free N_2, the irradiation in the target chamber produced activity bearing particles. The mean particle diameter was about $20nm$ and the total number concentration was in the order of $8000 particles/cm^3$ for a reactor power of $100kW$. This result was tentatively explained by radiopolymerisation of impurities in the N_2. The size distribution of KCl-particles did not change by irradiation at least for a reactor power of $100kW$. This important question will be adressed with heavy ion beams at the UNILAC at much higher energies and projectil intensities.

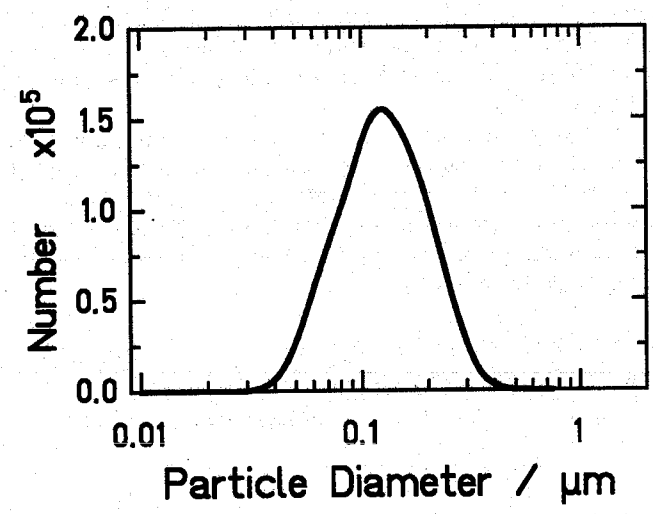

Figure 2: Logarithmic distribution of particle number vs. particle size (diameter)

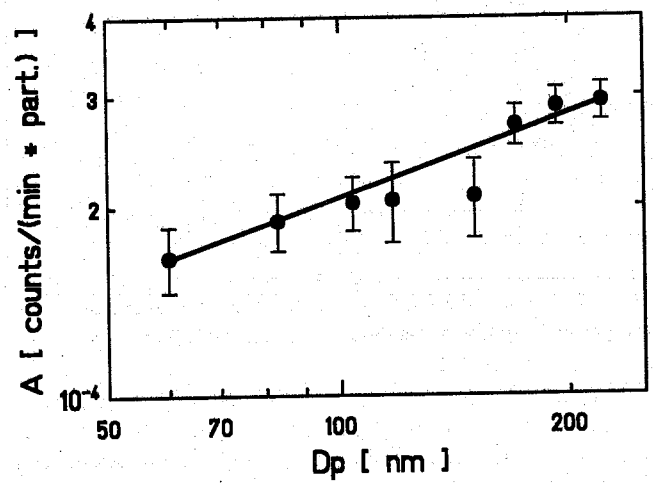

Figure 3: Attached ^{99}Nb activity per particle vs . particle diameter

References

[1] Hinds, W.C., Aerosol Technology, Wiley & Sons , New York, 272-278
[2] A. Weber, PSI-Report Nr.129, ISSN 1019-0643
[3] Schmidt-Ott et al, J. Aerosol Sci. 21, 711-717

Batch Experiments with Carrier Free Hf on Cation Exchange Resin DOWEX 50X8 in HCl/HF Containing Aqueous Solutions G+B

D. Schumann, S. Fischer, St. Taut: Technische Universität Dresden, FRG
A.F. Novgorodov, R. Misiak, N.A. Lebedev: JINR Dubna, Russia

Introduction: It was shown that HCl-HF is a useful medium to separate Hf, W and Lu on strongly acidic cation exchangers.[1] In the present work we study in detail the behaviour of Hf in this system in order to find conditions for the separation of the elements 104-106.[2,3]

Experimental: Carrier free Hf-175, -179, -181 was produced by irradiation of Re with 650 MeV protons at the phasotron "F" (Laboratory for Nuclear Problems, JINR Dubna). The target was dissolved in 6 M HNO_3. For the separation from Re the r. e. elements and Hf were adsorbed on DOWEX 50X8 and eluated with 6 M HCl. After evaporatiing the eluate to dryness the residue was solved in conc. HCl and adsorbed on DOWEX 1x8. The r. e. elements were separated by washing the column with 10 M HCl. After this procedure Hf was eluated with 8 M HCl.

All experiments were carried out by shaking 5 ml radioactive Hf containing solution with 200 mg of DOWEX 50x8 (20-50 mesh) for one hour (kinetic experiments differed only in sorption time). The radiation of Hf in aliquots of the liquid phase was measured by using a Ge(Li)-detector.

Results and discussion: As can be seen from fig.1 it takes only 5 minutes to attain the equilibrium.

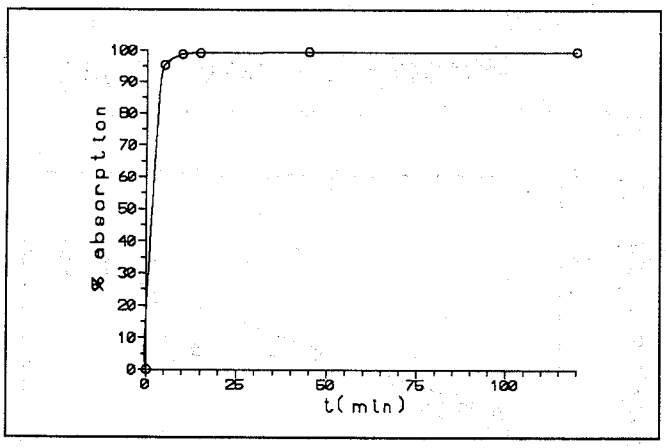

Fig. 1: Adsorption of Hf on DOWEX 50X8 in 10^{-4} M HF containing 0.1 M HCl in dependence on time; T = 298 K

In 0.1 M HCl and 10^{-4} M HF only 1 % Hf remains in solution. This is in good agreement with stability constants of Hf fluorides and hydroxides[4,5] as a calculation shows (fig. 2).[6]

The sorption of Hf decreases with increasing HF concentration. It reaches 0 at about 10^{-2} M HF (fig 3.).

The dependence of the sorption on the HCl concentration (0.1 M, 0.5 M) is surprising. Since the protonation of fluoride is lower at lower pH values and therefore the concentration of free F^- is higher, one should expect a sorption decrease with decreasing pH due to complex formation with fluoride, however the actual behaviour is opposite. This phenomenon requires further investigation.

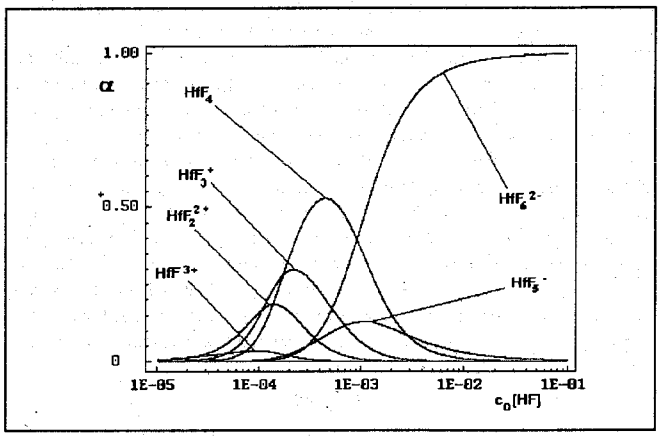

Fig. 2: Hf fluorid species in HF solutions containing 0.1 M HCl

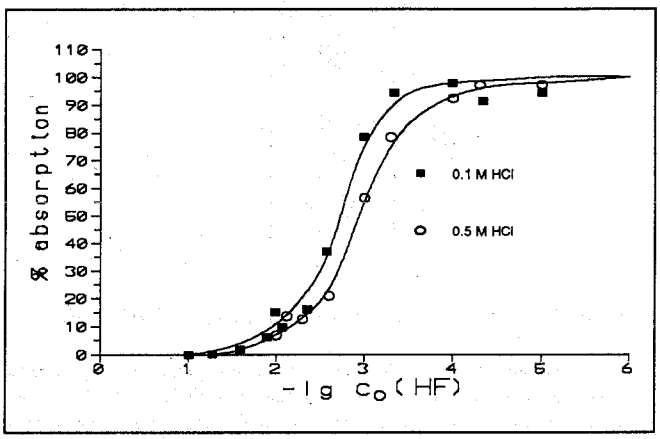

Fig. 3: Adsorption of Hf on DOWEX 50X8 depending on HF concentration; T = 298 K

Conclusions: Considering the different behaviour of Ta[7] the system in question can be used to separate Hf and Ta. In order to be applicable to separation of very heavy elements (in this case elements 104/105) this model has to be verified under high speed dynamical conditions.

1 S. Fischer et. al., GSI-Report No. 92-1 (1992) 316
2 H. Bruchertseifer, thesis, Leipzig 1982
3 H. Bruchertseifer, ZfI-Mitteilungen 165 (1991) 6
4 P.O. Virtanen, R. Kerkelä, Suomen Kem. 42 (1969) b29
5 V.M. Peshkova, P. An, Zhur. neorg. khim. 7 (1962) 2110
6 St. Taut, program KURVSIM, thesis, Dresden 1993
7 S. Fischer, D. Schumann et. al., to be published

Sorption of Carrier-free ^{95}Zr(IV)- and ^{95}Nb(V)- Isotopes from HCl/HF-Solutions on Dowex 50Wx8 and Dowex 1x8 G+B

A. Roß, S. Fischer, St. Taut, H. Bruchertseifer [2]
Technische Universität Dresden; [2] Paul Scherrer Institut, Villigen

Introduction: The ion exchange behaviour of Zr and Nb on Dowex 50 and Dowex 1 in HCL/HF solutions was studied in order to find appropriate conditions for experimental investigation of elements 104 and 105.

Experimental: ^{95}Zr and its daughter ^{95}Nb were separated with the method described in [1]. Dowex 50Wx8 and Dowex 1x8 were prepared and transferred into $[H^+]$- cf. $[Cl^-]$-form according to [2a]. Fresh prepared HCl/HF-solutions containing ^{95}Zr(IV) and ^{95}Nb(V) were used.

1. Sorption from HCl solutions (fig 1): On Dowex 1 **Zr** shows small sorption up to 5 M HCl. In these solutions cationic and neutral species are dominant. At higher HCl concentrations the sorption increases due to the formation of anionic complexes $ZrCl_5^{2-}$ and $ZrCl_6^{2-}$. On Dowex 50 sorption decreases with increasing acid concentration. Arising sorption in concentrations > 8 M HCl are a result of resin property changes.[2b]

Nb forms in solutions with > 4 M HCl anionic complexes (supposed as $NbOCl_4^-$ and $Nb(OH)_2Cl_5^{2-}$). It's sorption on Dowex 1 has a minimum at 4 M HCl. Increasing sorption in lower HCl concentrations is known from literature (physical adsorption of hydrolysed species).[3] No sorption occurs in 2 M HCl on Dowex 50 due to the formation of neutral compounds ($NbOCl_3$ or $Nb(OH)_2Cl_3$).

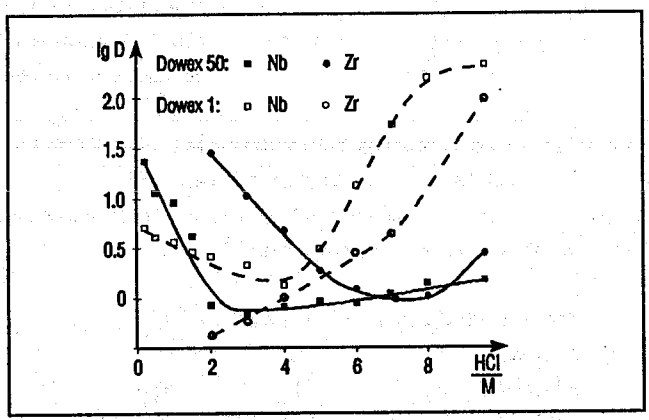

Fig. 1: Distribution coefficient D as a function of HCl concentration, 298 K

2. Sorption from HCl/HF solutions: A systematic investigation of sorption in HCl/HF solutions (included inert salt effects) was carried out in [4]

2.1. HCl solutions containing variable HF concentrations (fig. 2): On Dowex 1 **Zr** is not adsorbed at HF concentrations < $5 \cdot 10^{-5}$ M HF. According to equilibrium simulation [5] with literature data [6] cationic and neutral compounds are assumed. An increasing sorption is observed when fluoride concentration grows up caused by arising formation of anionic fluoride complexes (mainly ZrF_5^-).

Distribution results on Dowex 50 correspond with the tendency described for the anionite, at $5 \cdot 10^{-3}$ M HF mainly neutral ZrF_4 exists which is almost not adsorbed.

Only few references are dealing with Nb fluoride complex formation. In contrast to Zr the Nb fluorides are oxo compounds. Formation of neutral and anionic Nb compounds needs less fluoride than Zr. In comparison with Zr higher sorption of Nb on Dowex 1 is observed. The behaviour of Nb with Dowex 50 agrees with that of the anionite.

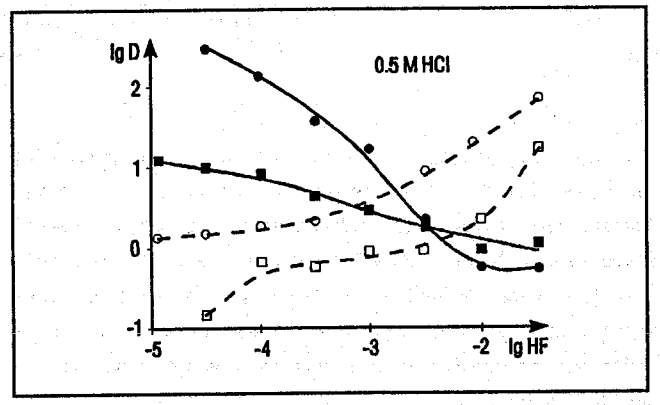

Fig. 2: Distr. coeff. D as a function of HF conc., 298 K; legend: ref. fig. 1.

2.1. HF solutions containing variable HCl concentrations (fig. 3): Depending on HCl concentration the free fluoride concentration changes. Consequently, a decrease of distribution coefficient on Dowex 1 occurs with arising HCl concentration. The separation of Zr and Nb doesn't improve notably. Also on Dowex 50 smaller sorption rates were observed.

Conclusions: Separation of Zr and Nb is possible under the following conditions: Dowex 50 and 0.1 M HCl/$5 \cdot 10^{-4}$ M HF, in this medium Zr is fixed at the exchanger, Nb remains in solution. Zr can be quantitatively eluated using solutions with high HCl and HF concentrations. At Dowex 1 a separation is possible using a 0.5 M HCl/0.01 M HF mixture. Nb is hold at resin and Zr remains in solution. These conditions were successfully transferred to column separation, they should be applied in further experiments to high speed on line methods for example ARCA II.[7]

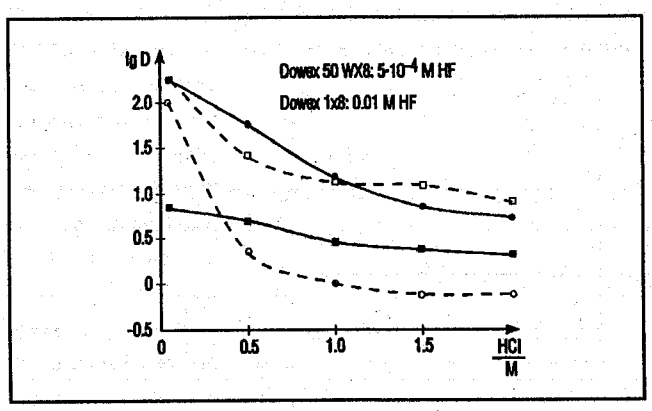

Fig. 3: Distr. coeff. D as a function of HCl conc., 298 K; legend: ref. fig. 1

1 R. H. Huffmann et. al., J. Amer. Chem. Soc. 73 (1951) 4474
2 M. Marhol: Ion exchangers in analytical chemistry, Publ. house "MIR", Moscow 1985, p. 76 (2a), p.494 (2b) (russ.)
3 L. R. Bunney et. al., Anal. Chem. 31 (1959) 324
4 A. Roß, thesis, TU Dresden 1992 (german)
5 St. Taut, PhD thesis, TU Dresden 1993 (german)
6 E. Högfeld(Editor): Stability constants of metal-ion complexes, IUPAC Chem. Data Series No. 21, Pergamon Press, London 1982
7 M. Schädel et. al., Radiochimica Acta 48 (1989) 171

Thermochromatography of Californium, Einsteinium, and Fermium in Metallic Columns[B]

S.Hübener
Institut für Radiochemie, Forschungszentrum Rossendorf e.V.
B.Eichler, H.Gäggeler
Paul Scherrer Institut, Villigen, Switzerland
M.Schädel
GSI, Darmstadt

Thermochromatography in metal columns is a promising technique for the fast separation of heavy actinoids. However, analytical applications were limited due to admixtures of calcium, added in weighable amounts to stabilize the trace amounts to be separated in the elementary state[1]. In an earlier attempt to study the heavy actinoids under calcium-free conditions vacuum-thermochromatography has been used[2].

In the present work the heavy actinoid fraction of experiments carried out to investigate further the chemical properties of element 105 at the UNILAC of the GSI[3] was used to study the thermochromatography of Cf, Es, and Fm in titanium, molybdenum, and tantalum columns under calcium-free conditions using high-purity helium as a carrier gas. The experimental procedure was very similar to that described earlier in detail[1]. The actinoids under study were evaporated from a lanthanum/aluminium melt into a titanium pre-column. At 1275 K the evaporated actinoid atoms entered with the carrier gas the open tubular thermochromatographic column. The column was held at working temperature for 30 minutes. The distribution of the actinoids was measured off-line by alpha spectrometry in 1 cm sections. Among others ^{248}Cf, ^{249}Cf, ^{252}Es, ^{253}Es, and ^{255}Fm were used as the indicatory isotopes. A schematic of the columns used and the thermochromatographic distribution in titanum and molybdenum columns are shown in Fig.1 and Fig.2, respectively. On molybdenum and tantalum Cf and Es were deposited immediately after having left the pre-column, obviously at the first contact with the metallic surface.

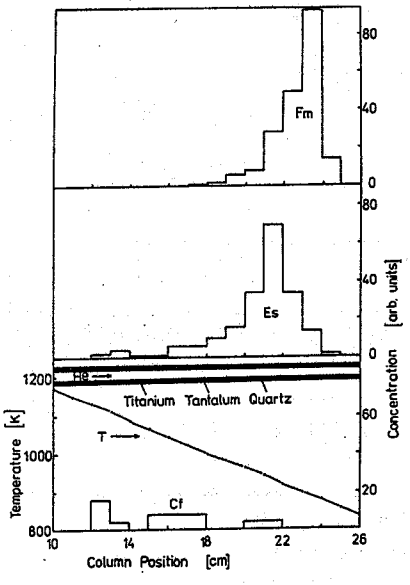

Figure 1: Thermochromatographic distribution of Cf, Es, and Fm in a titanium column.

Fm was deposited at 1225 K on molybdenum and at 1200 K on tantalum. In titanium columns Es and Fm were transported down to 930 K and 890 K, respectively, whereas Cf was lost due to diffusion into the titanium bulk. Enthalpies of adsorption evaluated from the experimental data are summarized in Table 1. Theoretical enthalpies of ad-

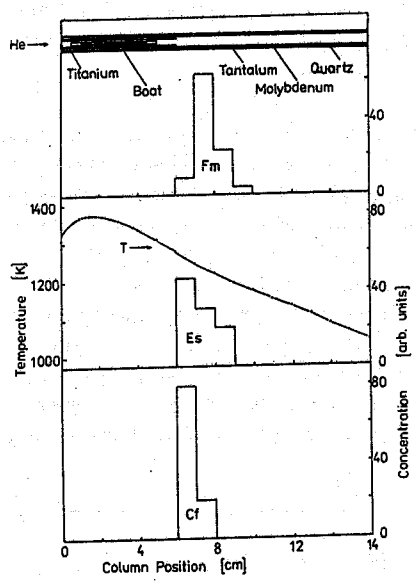

Figure 2: Thermochromatographic distribution of Cf, Es, and Fm in a molybdenum column.

sorption on titanium calculated on the basis of an empirical model are given for comparison[4].

Table 1: Enthalpies of adsorption H_{ads}

Actinoid	Cf	Es	Fm
Adsorbens metal	H_{ads} [kJ/mol]	H_{ads} [kJ/mol]	H_{ads} [kJ/mol]
Mo	307.9	301.3	290.6
Ta	302.1	302.1	277.3
Ti	Diffusion	219.2	210.2
$Ti_{(calc)}$	283.4	214.7	210.4

As follows from these data also under calcium free conditions titanium can be used as a column material for the gaseous phase transport of Es and Fm at temperatures above 1000 K and for their chromatographic separation. Thermochromatographic studies in columns made of metals like Mo, Nb, and Ta should be continued at higher temperatures.

[1] S.Hübener, I.Zvara, Radiochim. Acta 31, 89 (1982)
[2] B.Eichler et al, Kernenergie 30, 469 (1987)
[3] A.Türler et al., contribution to this report
[4] B.Eichler, S.Hübener, H.Roßbach, Report ZfK-560 (1985)

ON-LINE ISOTHERMAL GAS CHEMISTRY EXPERIMENTS WITH CHLORIDES OF ELEMENT 105

H.W. Gäggeler, B. Eichler, D.T. Jost, A. Kovacs, D. Vermeulen
Paul Scherrer Institut, Villigen

A. Türler, B. Kadkhodayan, K.E. Gregorich, S.A. Kreek, D.M. Lee, D.C. Hoffman
Lawrence Berkeley Laboratory, Berkeley

P. Baisden
Lawrence Livermore National Laboratory, Livermore

J.V. Kratz, H.-U. Becker, H.P. Zimmermann
Institut für Kernchemie der Universität Mainz

M. Schädel, W. Brüchle, E. Jäger, V. Pershina, B. Schausten, E. Schimpf
GSI Darmstadt

Relativistic alterations of the electronic structure might modify the chemical properties of very heavy elements compared to their lighter homologues. The chemistry of the transactinide elements has, therefore, gained broad interest from both experimental and theoretical chemists[1]. In 1990 we studied the volatility of element 105 bromides,[2] now we have extended our studies to the 105 chlorides.

We have used the **H**eavy **E**lement **V**olatility **I**nstrument[3] (HEVI) and the **O**n-**L**ine **G**as chemistry **A**pparatus[4] (OLGA) to investigate the volatility of element 105 chlorides and their homologues by isothermal gas chromatography in empty quartz columns. 34-s ^{262}105 and 27-s ^{263}105 were produced at the UNILAC accelerator at GSI by bombarding a freshly prepared target of ^{249}Bk with an intense beam of 99 MeV ^{18}O. ^{262}105 decays by 67% α-emission and 33% spontaneous fission (SF), whereas ^{263}105 decays by 43% α-emission and 57% SF.[5]

Reaction products, transported by a He/MoO_3 aerosol gas jet, were continuously collected on a quartz wool plug kept at 900 °C before the isothermal section of the quartz chromatography column. The chlorides of element 105 were formed by adding 160 ml/min Cl_2 gas saturated with CCl_4. Volatile species were carried to the cooler, isothermal section of the column by the He flow. In the isothermal part of the column the retention behaviour of the chlorides was studied as a function of the temperature. Behind the quartz column, the molecules passing through the column were reattached on KCl aerosol particles, and transported through a capillary to the counting device, a modified magnetic tape station. Here, in a collection chamber the products were deposited on the surface of a conventional computer tape[4]. Every 20 s the tape was stepped to subsequently transport the activity in front of six 450 mm^2 PIPS detectors for α- and SF-counting. In addition to the activities of ^{262,263}105 and their daughters ^{258,259}Lr, lines due to Po and Bi isotopes were visible, which were produced from small lead impurities in the ^{249}Bk target. Unfortunately our experiments were hampered by low gas jet transport efficiencies.

The analysis of these experiments is still in progress and only preliminary results will be reported here. A decay curve analysis (Fig. 1) of SF-activities observed in all gas chemistry runs at a beam energy of 99 MeV resulted in a half-life of 47^{+11}_{-8}s, assuming a minor contamination with ^{256}Fm(^{256}Md). This half-live is somewhat long compared to the literature value, but agrees well with the 44^{+19}_{-12} s half-life observed in earlier gas chemistry experiments.[2]

The analysis of α-spectra revealed 7 correlated α–α pairs, which resulted from the decay of 34-s ^{262}105 and its 3.93-s ^{258}Lr daughter. Half-lives of 28^{+17}_{-8} s and $3.8^{+2.3}_{-1.0}$ s resulted for the mother and the daughter nuclides, respectively, in good agreement with the literature values. The observation of correlated mother-daughter pairs can be regarded as unambiguous proof, that element 105 was observed after chemical separation. The chemical yield of 105-chlorides at an isothermal temperature of 80 °C was considerably lower than that measured at 250 °C and higher temperatures. This indicates, that the 105 chlorides are more volatile than 105 bromides,[2] probably similar in volatility to $NbCl_5$.[6]

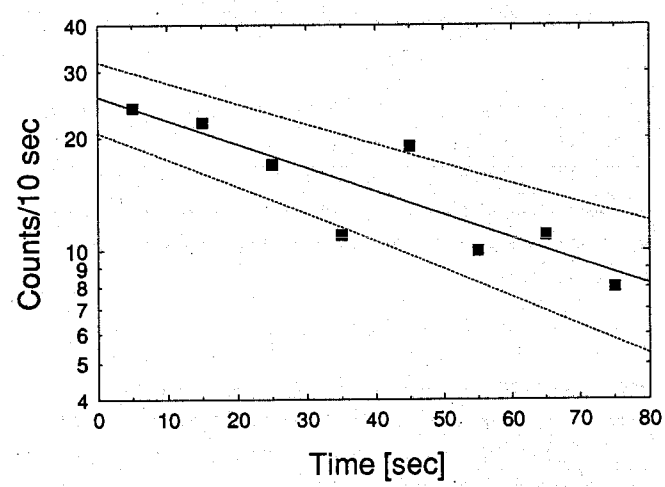

Figure 1: Decay curve of SF-decays observed in all gas chemistry runs at the 99 MeV beam energy. The centre curve is the most probable fit to the data assuming a short-lived SF activity (47^{+11}_{-8} s) and a long-lived contaminant ^{256}Fm(^{256}Md). The dashed lines encompass 68% of the probability in a Poisson distribution centred on the number of counts in the most probable fit.

1 V. Pershina et al., J. Chem. Phys., 96, 8367 (1992)
2 H.W. Gäggeler et al., Radiochim. Acta, 57, 93 (1992)
3 B. Kadkhodayan et al., Nucl. Instr. Meth., A317, 254 (1992)
4 H.W. Gäggeler et al., Nucl. Instr. Meth., A309, 201 (1991)
5 J.V. Kratz et al., Phys. Rev. C45, 1064 (1992)
6 B. Kadkhodayan, Progress Report 1992, Annex III, Paul Scherrer Institut (1993)

Active Pressure of Atomic Nb, Ta, and Ha as a Function of Electronic Configuration

V. Pershina, B. Fricke
Theoretical Physics Department, University of Kassel
G. V. Ionova
Institute of Physical Chemistry, Russian Academy of Sciences, Moscow
E. Johnson
Chemistry Division, Oak Ridge National Laboratory

Studying the volatility of the heavy elements as a function of their electronic configurations has been of a high experimental interest.[1,2] In the present work the volatility of element 105 as a function of electronic configuration and temperature has been analyzed, and in relation to the analogs Nb and Ta.

Volatility or active pressure f_i of a component i is a function of pressure, temperature and concentration c_i of this component, $f_i = function\ (p_i, T, c_i)$. At T = const, $d \ln f_i = (d\mu_i)_T/RT$, where μ_i is the chemical potential. For a monatomic ideal gas with statistical weight g_k

$$\mu_i = T \ln\left[\frac{N_i}{Z_i V_i} \left(\frac{2\pi\hbar^2}{m_i T} \right)^{3/2} \right] , \qquad (1)$$

where the partition function Z_i is

$$Z_i = \sum_k g_k e^{-\Delta\varepsilon_k/T} = \sum_J (2J+1) e^{-\Delta\varepsilon_J/T} . \qquad (2)$$

$\Delta\varepsilon_J$ is the energy difference between the fine-structure components (different in the values of J).

In this work we have considered the relationship f_1/f_2 for the following cases: when atoms of one element differ by their electronic configurations and when there are different elements. In the first case

$$f_1/f_2 = Z_2(T)/Z_1(T) . \qquad (3)$$

We considered element 105 in electronic configurations d^3s^2, d^3sp, and d^4s respectively. To calculate the partition functions Z_1 and Z_2, the MCDF calculations of the lowest energy states that are dominated by these configurations as a function of the total angular momentum quantum number have been performed for Ha (and V, Nb, Ta), so that

$$Z_1(Ha_1,\ d^3s^2) = 4 + 6e^{-\frac{4746}{T}} + 8e^{-\frac{8149}{T}} + 10e^{-\frac{10011}{T}}$$

$$Z_2(Ha_2,\ d^4s) = 2 + 4e^{-\frac{1023}{T}} + 6e^{-\frac{3851}{T}} + 8e^{-\frac{6060}{T}} + 10e^{-\frac{7657}{T}} .$$

The resultant values of Z_1/Z_2 and f_1/f_2 show that up to $\simeq$ 1500 K element 105 would be more volatile in electronic configuration d^4s than in d^3s^2 and this relation is reversed at higher temperatures. The partition function for the d^3sp configuration is

$$Z_3(Ha_3,\ d^3sp) = 4 + 6e^{-\frac{4815}{T}} + 8e^{-\frac{7387}{T}} + 10e^{-\frac{9429}{T}} + 12e^{-\frac{14251}{T}}$$

At the temperatures higher than 2000 K hahnium in the electronic configuration d^3s^2 starts to be more volatile than in the electronic configuration d^3sp.

These results show an important competition between d^4s, d^3sp and d^3s^2 configurations and their influence on the volatility.

For the volatility of different elements (second case):

$$f_1/f_2 = [m_2^{3/2} Z_2(T)]/[m_1^{3/2} Z_1(T)] . \qquad (4)$$

At low temperatures the volatility in accordance with eq 4 is determined by the mass effect, thus $f_{Ta}/f_{Ha} = 1.98$. When temperature increases the volatilities of Ta and Ha become equal. The increase in volatility of a heavier element compared to a lighter one is due to the fact that in the heavy elements the large spin-orbital effect decreases Z thus compensating for the large mass in relation 4. As a result, the heavier element can be more volatile than the lighter one with increasing temperature.

Assuming that Ha has the same structure in the metallic state as Ta having the bcc lattice and configuration $d^{4-x}sp^x$, we have estimated its sublimation enthalpy using the expression[3] $\Delta H_{subl} = E_b - \Delta E$, where E_b is the valence state bonding energy of the metal and ΔE (obtained from the MCDF calculations) is the difference between the energy of the ground state electronic configuration realized in the gas phase and the energy of the exited state configuration realized in the condensed state. Thus $\Delta H_{subl} \simeq 10.2 \pm 0.4$ eV.

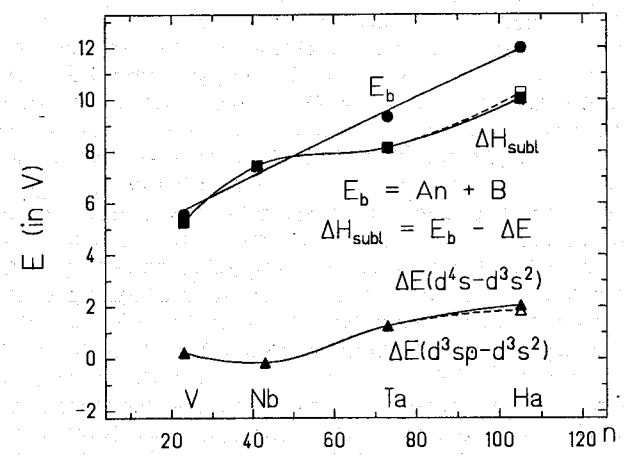

Fig.1: Sublimation energy of a metal ΔH_{subl}, binding energy E_b and the difference between energies of electronic configurations $\Delta E(d^4s - d^3s^2)$ (filled triangles) and $\Delta E(d^3sp - d^3s^2)$ (open triangle for Ha) as a function of the atomic number.

1. Jost, D. T.; Gäggeler, H. W.; Vogel, Ch.; et al., Inorg. Chim. Acta 146, 255, (1988).
2. (a) Zhuikov, B. L.; Chuburkov, Yu. T.; Timokhin, S. N.; Zvara, I. Radiochim. Acta 46, 113, (1989) (b) Eichler, B.; Hübener, S.; Gäggeler, H. W.; Jost, D. T. Inorg. Chim. Acta 146, 261 (1988).
3. Brewer, L. J. Opt. Soc. Am. 61, 1101, (1971).

4.2

The Complex Formation of Element 105 in Aqueous HCl Solutions, Electronic Structure of Anionic Chloride Complexes

V. Pershina, B. Fricke
Theoretical Physics Department, University of Kassel
G. V. Ionova
Institute of Physical Chemistry, Russian Academy of Sciences, Moscow

A series of the extraction chromatography experiments[1] studied the halide complexation of element 105 under conditions where Nb, Ta, and Pa are extracted into triisooctyl amine (TIOA). The results have shown that the anionic halide complexes of Ha are different from those of Ta, and are more like those of Nb and Pa.

In the present work relativistic Dirac-Slater molecular orbital calculations have been performed for the for $[MCl_6]^-$, $[M(OH)_2Cl_4]^-$, and $[MOCl_5]^{2-}$ (M = Nb, Ta, Ha, and Pa) complexes with the aim to understand the role of different orbitals in the chemical bond formation and the differences in the halide complexing of the group 5 elements.

The calculations have shown that Ha has a characteristic of the d-elements scheme of the molecular levels, so that the trans-effect in the oxyhalide anions of Ha should be typical of the d elements and opposite to that in the actinides (Fig. 1). The different trans-effect in the actinide and d-element compounds is explained by different ordering of vacant MOs in these systems.[2] This causes the different vibrational modes (T_{1u} and E_g) to be active thus giving rise to the different geometrical distortions of the octahedral systems.

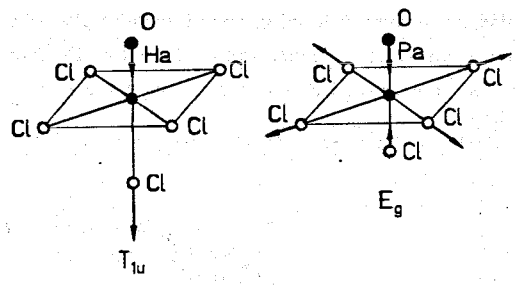

Fig. 1. Different trans-effect in the octahedral complexes of the d elements and actinides (T_{1u} and E_g are different vibrational modes).

The molecular orbital eigenvalues show the increasing crystal-field splitting of the valence d orbitals in going from $[NbOCl_5]^{2-}$ to $[TaOCl_5]^{2-}$, and to $[HaOCl_5]^{2-}$. A relative decreasing in energy of the highest unoccupied levels in the hahnium complexes is due to a large contribution of the relativistically stabilized 7s AOs.

The Mulliken population analysis has been applied to study the tendency of a metal to form covalent bonding with particular ligands and their number (or coordination). Analysis of the involvement of the valence orbitals in bonding has shown that the d orbitals participation increases steadily from Nb to Ta and to Ha, while 7s AOs are less accessible for Cl (in terms of bonding) in case of Ha than the 6s ones in case of Ta (for single bonds). Destabilization of the $7p_{3/2}$ orbitals in Ha complex is so large that their overlap with chlorines is even less than the overlap $5p_{3/2}$ - Cl in Nb complex.

The change in the relative values of the covalent bonding $n(M\text{-}Cl_{eq})/n(M\text{-}Cl_{ax})$ (n is a partial overlap population) in going from Nb to Ta influences the trans-effect in these complexes. Increase in the covalent bonding $M\text{-}Cl_{eq}$ in Ha complex results in decreasing the trans-effect on the coordinate Cl_{ax}-Ha-O, so that the oxygen atom is bound stronger and less easily substituted. Ta has the highest covalency of the bond $M\text{-}Cl_{ax}$, and the strongest trans-effect, what means that the substitution of oxygen in $[TaOCl_5]^{2-}$ should be the most easily reached.

The advantage of an element to form oxyhalide or pure halide complex in terms of the covalent bonding can be seen from the Table.

Table. Total overlap population data (covalent bonding) for $[MCl_6]^-$ and $[MOCl_5]^{2-}$ complexes

n(M - L)	$[NbCl_6]^-$	$[TaCl_6]^-$	$[HaCl_6]^-$	$[PaCl_6]^-$
M - Cl	0.42	0.50	0.49	0.42
M - 6Cl(tot)	2.52	2.97	2.95	2.51
n(M - L)	$[NbOCl_5]^{2-}$	$[TaOCl_5]^{2-}$	$[HaOCl_5]^{2-}$	$[PaOCl_5]^{2-}$
M = O	0.78	0.88	0.92	0.83
$M\text{-}Cl_{eq}$	0.34	0.39	0.42	0.36
$M\text{-}Cl_{ax}$	0.36	0.40	0.36	0.28
M - L (tot)	2.51	2.85	2.96	2.57

Thus tantalum shows the clear preference to form pure halide complexes, it has much higher overlap with six chlorines than when one chlorine is substituted by oxygen. For niobium and hahnium the trends to form oxyhalide and halide complexes are nearly equal (for Ha there is more pronounced trend to form oxyhalide species). The small overlap of the ns and $np_{3/2}$ orbitals with chlorines in the $[HaCl_6]^-$ complex leads to the total overlap metal-ligand being not larger than in the $[TaCl_6]^-$.

Thus, the results of the calculations show qualitatively the trends found in the experiments: there is a specific position of Ta in the group and the preference to coordinate 6 or 7 chlorines, while Pa and Ha have a tendency to form rather oxyhalide complexes $[MOCl_5]^{2-}$ at high HCl concentrations, or, probably, $[HaCl_7]^{2-}$ at even higher molarities.

1. J. V. Kratz, H. P. Zimmermann, U. W. Scherer, et al., Radiochim. Acta 48, 121 (1989).
2. G. V. Ionova, V. G. Pershina, V. I. Spitsyn, "The Electronic Structure of the Actinides", Nauka, Moscow, 1986 (in Russian).

Theoretical Consideration of the Anionic Exchange of the Group 5 Elements in the Extraction with Aliphatic Amines

V. Pershina, B. Fricke
Theoretical Physics Department, University of Kassel
G. V. Ionova
Institute of Physical Chemistry, Russian Academy of Sciences, Moscow

Molecular orbital calculations[1] of the halide and oxyhalide anionic complexes of the group 5 elements using the Dirac-Slater Discrete Variational Method have shown that Ha has a trend to form oxyhalide complexes $[HaOCl_5]^{2-}$ like $[NbOCl_5]^{2-}$ and $[PaOCl_5]^{2-}$ at high HCl concentrations rather than pure halide ones, e.g. $[HaCl_6]^-$, which are typical of Ta. In this work we try to estimate the possible behaviour of element 105 in the solvent extraction from aqueous HCl solutions into triisooctylamine (TIOA) on the basis of the results of these calculations and the atomic Multiconfiguration Dirac-Fock (MCDF) ones.[2] The consideration was restricted to the high HCl concentrations.

The process of the extraction of a metallic species M^{z+} by the amine can be subdivided into two steps. In the first step, the complex anion ML_n^{z-n} is transferred from the aqueous into the organic phase together with an equivalent amount of large organic cation R_3NH^+:

$$ML_{n,aq}^{z-n} + (n-z)R_3NH_{aq}^+ \rightarrow ML_{n,org}^{z-n} + (n-z)R_3NH_{org}^+ \qquad (1)$$

And the second stage is the ion-associating in the organic phase:

$$ML_{n,org}^{z-n} + (n-z)R_3NH_{org}^+ \rightarrow [(n-z)R_3NH^+ML_n^{z-n}]_{org}^0 \qquad (2)$$

The work of transfer of the anion can be expressed according to the Born's theory of solubility[3]

$$W_t = -W_{aq} + W_{org} = \frac{Z_i^2 e^2}{2r_i}\left(\frac{1}{\varepsilon_{org}} - \frac{1}{\varepsilon_{aq}}\right) \qquad (3)$$

Here Z_i is the number of unit charges on the ion, r_i - the radius of the ion, and ε_{org} and ε_{aq} are dielectric constants of the organic and aqueous phases, respectively.

Usually $\varepsilon_{org} < \varepsilon_{aq}$, so that the change of the free energy is positive: $\Delta G_t = W_t > 0$. The sign of the free energy change remains still positive even if the ionic association in the organic medium takes place.

For the associating of the ions in the organic phase the Bjerrum's theory[4] gives the expression for the association constant

$$K_{ass} = \frac{4\pi N}{1000}\left(\frac{Z_1 Z_2 e^2}{\varepsilon_{org} kT}\right)^2 Q(b) \;, \quad b = e^2/q\varepsilon_{org}kT \;, \qquad (4)$$

where ε_{org} is a dielectric constant, Z_1 and Z_2 are ionic charges and $q = r_1 + r_2$ is a distance of closest approach of the ions. The free energy of the ion association is then $\Delta G_{ass} = -RT \ln K_{ass}$.

The partition coefficient is $P = C_{org}/C_{aq}$, where C_{org} and C_{aq} are concentrations of the species in the aqueous and organic phases. And finally it can be expressed as

$$P = \frac{C_{org}}{C_{aq}} = \frac{\gamma_{aq}}{\gamma_{org}} \exp\left[\frac{Ne^2 Z_i^2}{2RTr_i}\left(\frac{1}{\varepsilon_{org}} - \frac{1}{\varepsilon_{aq}}\right)\right]. \qquad (5)$$

Assuming that Nb, Pa, and Ha form similar oxyhalide species $[MOCl_5]^{2-}$, the size of each can be estimated on the basis of the ionic radius, which for Ha was obtained from the MCDF calculations.[2] Having $r(NbOCl_5^{2-}) < r(HaOCl_5^{2-}) < r(PaOCl_5^{2-})$, the partition of the anionic species under consideration between the organic and aqueous phases will be (see Fig. 1).

$$P(NbOCl_5^{2-}) > P(HaOCl_5^{2-}) > P(PaOCl_5^{2-}) \qquad (6)$$

The knowledge of the sizes of the anions under consideration is also important for the estimation of q in Eq. (4). The estimated values are 7.78, 7.85, and 7.92 Å for complexes of Nb, Ha, and Pa, respectively. Using these values the strength of the associated complexes due to the electrostatic interaction will be:

$$K_{ass}(NbOCl_5^{2-}) > K_{ass}(HaOCl_5^{2-}) > K_{ass}(PaOCl_5^{2-}) \qquad (7)$$

The hydrogen bonding will not change the trend obtained from the electrostatic model. A critical value of the dielectric constant ε_{org} has been determined as 40, above which there will be no association in the organic phase.

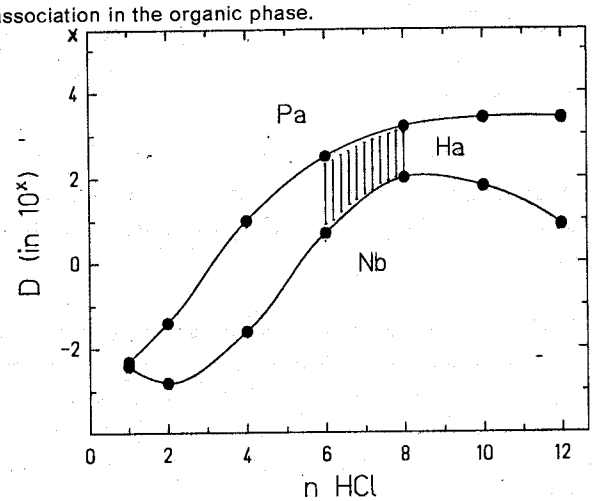

Fig. 1. The distribution coefficient between the TIOA and aqueous phase. (The Pa and Nb are literature data[5], Ha are estimated values).

1. V. Pershina, B. Fricke, G. V. Ionova, sub. to Inorg. Chem.
2. E. Johnson and B. Fricke, Radiochim. Acta (to be published).
3. M. Born, Z. Physik, 1, 45 (1920)
4. N. Bjerrum, K. Danske Vidensk, 7, N 9 (1926)
5. Y. Markus and A. S. Kertes, Ion exchange and solvent extraction of metal complexes, 1969, p. 960.

Basic Thermodynamic Functions for Element 105 in a Neutral and in Ionized States

V. Pershina, B. Fricke
Theoretical Physics Department, University of Kassel
G. V. Ionova
Institute of Physical Chemistry, Russian Academy of Sciences, Moscow
E. Johnson
Chemical Division, Oak Ridge National Laboratory

The basic thermodynamic functions, the entropy, free energy and enthalpy for element 105 in electronic configurations d^3s^2 and d^4s^1 and for its +5 ionized state ($5f^{14}$) have been calculated as a function of temperature. The data are based on the results of the calculations of the corresponding electronic states of element 105 using the multiconfiguration Dirac-Fock method.

The entropy of element 105 has been calculated using the formular of the translational entropy of an ideal gas:

$$S = N_0 k \left[\ln \frac{Z(2\pi mkT)^{3/2}kT}{h^3 P} + \frac{5}{2} \right] \qquad (1)$$

Here $N_0 = 6.022\ 10^{23}\ mol^{-1}$, $k = 1.380\ 10^{-23}\ JK^{-1}$, $P = 1\ atm = 1.013\ 25\ 10^{8}\ dyne\ cm^{-1}$, m is a mass of Ha equal to $266/N_0$, and $h = 6.626\ 10^{-34}\ Js$.

Z is an electron partition function. For a monoatomic ideal gas with statistical weight g_k for the electron states, the expression for Z is

$$Z_i = \sum_k g_k e^{-\Delta\varepsilon_k/T} = \sum_J (2J+1) e^{-\Delta\varepsilon_J/T} \qquad (2)$$

Here the summation is taken over all possible values of the total angular momentum J for all L and S states. $\Delta\varepsilon$ is the difference between energies of the ground and excited states in the fine structure spectrum (for a given J) of element 105.

The values of $\Delta\varepsilon$ have been obtained as a result of the multiconfiguration Dirac-Fock atomic calculations of the lowest energy states of element 105 that are dominated by the d^3s^2 and by the d^4s^1 electronic configurations, and of Ha^{5+} in ($5f^{14}$) configuration.

The values of the partition function can be used for calculating some other physico-chemical characteristics such, for example, as chemical potentials, active pressure of a component, etc.

The free energy for element 105 has been calculated using the formula

$$G = -N_0 kT \left[\ln \frac{Z(2\pi mkT)^{3/2}kT}{h^3 P} \right]. \qquad (3)$$

The enthalpy, H, can be calculated from the general expression

$$G = H - TS. \qquad (6)$$

The obtained thermodynamic functions for different temperatures are presented in the Table.

Table. The calculated values of the partition function Z, entropy S, free energy G, and enthalpy H for element 105 in electronic configurations d^3s^2, d^4s, and Ha^{5+} at some temperatures

Conf.	T K	Z	S $kJ\ mol^{-1}K^{-1}$	-G $kJ\ mol^{-1}$	H $kJ\ mol^{-1}$
$Ha(d^3s^2)$	273	4.000	188.05	45.664	5.673
	298	4.000	189.90	50.388	6.194
	323	4.000	191.56	55.159	6.714
	373	4.000	194.54	64.811	7.753
	423	4.000	197.17	74.610	8.792
	500	4.000	200.63	89.922	10.393
	750	4.003	209.08	141.220	15.590
	1000	4.006	215.05	194.267	20.786
	1500	4.065	223.61	304.229	31.179
	2000	4.200	229.86	418.140	41.572
$Ha(d^4s)$	273	2.016	182.36	44.107	5.673
	298	2.028	184.23	48.706	6.194
	323	2.041	185.98	53.359	6.714
	373	2.077	189.09	62.776	7.753
	423	2.356	192.77	72.749	8.792
	500	2.407	195.69	87.449	10.393
	750	2.557	205.36	138.430	15.590
	1000	2.943	212.42	191.703	20.786
	1500	3.677	222.77	191.703	31.179
	2000	4.388	230.22	191.703	41.572
$Ha^{5+}(5f^{14})$	273	1.000	176.53	42.517	5.673
	298	1.000	178.38	46.982	6.205
	323	1.000	180.04	51.439	6.714
	373	1.000	183.02	60.513	7.523
	423	1.000	185.65	69.736	8.793
	500	1.000	189.13	84.169	10.393
	750	1.000	197.55	132.586	15.576
	1000	1.000	203.53	182.748	20.781
	1500	1.000	211.96	286.759	31.179
	2000	1.000	217.94	394.275	41.618

The obtained values of the thermodynamic functions can be used to study the gas-phase chemistry of element 105 at high temperature rates.